Sedimentology (2003) **50,** 1035–1060 doi: 10.1046/j.1365-3091.2003.00592.x

Characterization and correlation of Upper Jurassic (Oxfordian) bentonite deposits in the Paris Basin and the Subalpine Basin, France

PIERRE PELLENARD*, JEAN-FRANCOIS DECONINCK*, WARREN D. HUFF†, JACQUES THIERRY‡, DIDIER MARCHAND‡, DOMINIQUE FORTWENGLER§ and ALAIN TROUILLER¶

**Morphodynamique continentale et côtière, UMR 6143 CNRS, University of Rouen, Department of Earth Sciences, 76821 Mont St Aignan Cedex, France (E-mail: Pierre.Pellenard@univ-rouen.fr)*

†University of Cincinnati, Department of Geology, PO Box 210013, Cincinnati, OH 45221-00, USA

‡Biogéosciences-Dijon, UMR 5561CNRS, Department of Earth Sciences, University of Burgundy, 6 bd Gabriel, 21000 Dijon, France

§Le Clos des Vignes, Quartier Perry, 26160 La Bégude de Mazenc, France

¶ANDRA, Parc de la Croix Blanche, 1–7 rue Jean Monnet, 92298 Châtenay-Malabry, France

ABSTRACT

Explosive volcanic activity is recorded in the Upper Jurassic of the Paris Basin and the Subalpine Basin of France by the identification of five bentonite horizons. These layers occur in Lower Oxfordian (*cordatum* ammonite zone) to Middle Oxfordian (*plicatilis* zone) clays and silty clays deposited in outer platform environments. In the Paris Basin, a thick bentonite (10–15 cm), identified in boreholes and in outcrop, is dominated by dioctahedral smectite (95%) with trace amounts of kaolinite, illite and chlorite. In contrast, five bentonites identified in the Subalpine Basin, where burial diagenesis and fluid circulation were more important, are composed of a mixture of kaolinite and regular or random illite/smectite mixed-layer clays in variable proportions, indicating a K-bentonite. In the Subalpine Basin, a 2–15 cm thick bentonite underlain by a layer affected by sulphate–carbonate mineralization can be correlated over 2000 km^2. Euhedral zircon, apatite and biotite crystals have been identified in all the bentonites. The geochemical composition of the bentonites in both basins is characterized by high concentrations of Hf, Nb, Pb, Ta, Th, Ti, U, Y, Zr and low concentrations of Cr, Cs and Rb. Biostratigraphical and geochemical data suggest that the thick bentonite in the Paris Basin correlates with the thickest bentonite in the Subalpine Basin, located 400 km to the south. These horizons indicate that significant explosive volcanic events occurred during the Middle Oxfordian and provide potential long-distance isochronous marker beds. Immobile element discrimination diagrams and rare-earth element characteristics indicate that the original ash compositions of the thickest bentonites correspond to a trachyandesitic source from a within-plate alkaline series that was probably related to North Atlantic rifting.

Keywords Bentonites, clay minerals, correlations, Oxfordian, palaeovolcanism, Paris Basin, Subalpine Basin of France.

INTRODUCTION

Callovian and Oxfordian clay deposits from the eastern part of the Paris Basin have been chosen by the French government as a future host formation for nuclear waste disposal and will initially host an underground research laboratory (ANDRA, 2000). The 130 m thick clay deposits were continuously cored and recovered from ANDRA borehole HTM 102 (Fig. 1A). High-resolution studies (Pellenard

© 2003 International Association of Sedimentologists

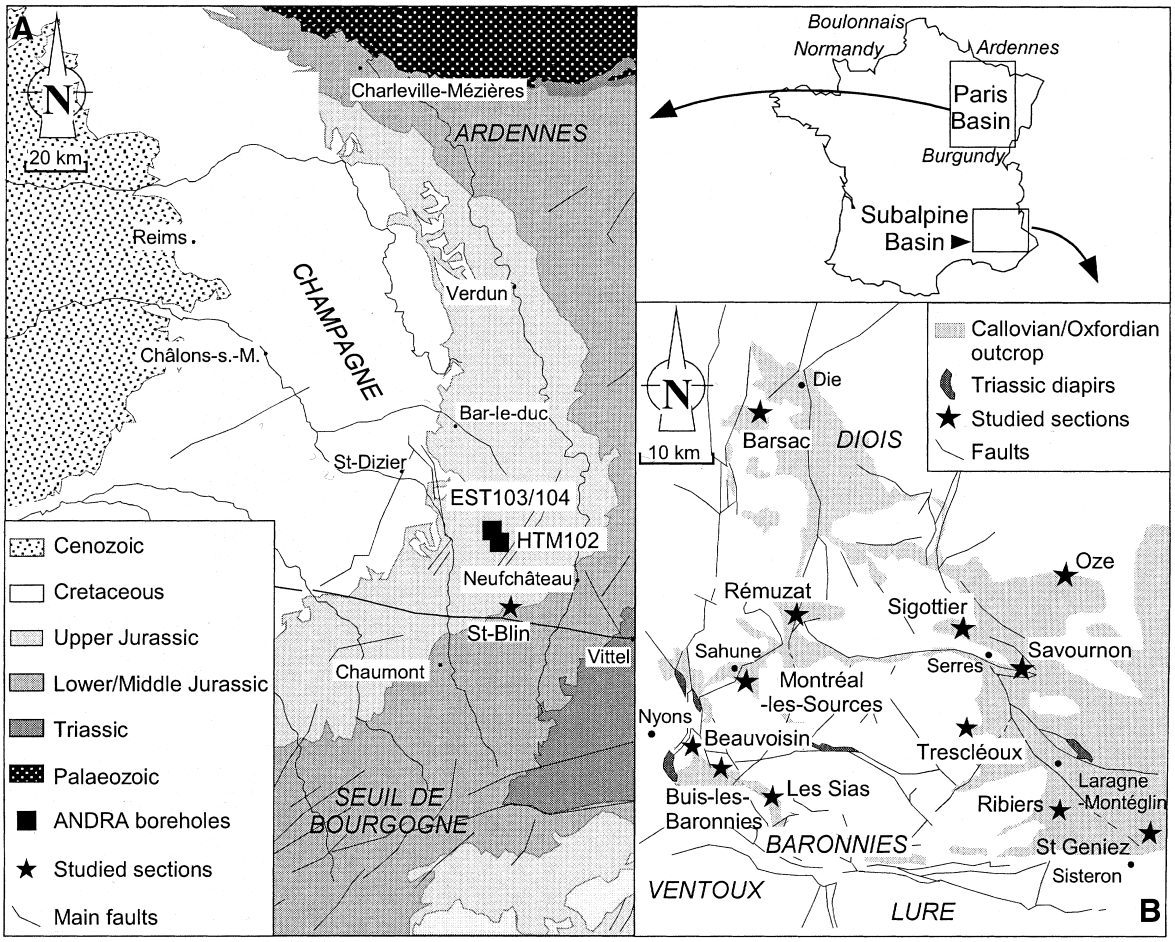

Fig. 1. Simplified geological maps and location of the studied outcrops and boreholes. (A) Eastern part of the Paris Basin. (B) Subalpine Basin.

et al., 1999) conducted through the cored section of the borehole (Fig. 2) have revealed:

1 a major mineralogical change occurring in the Lower Oxfordian (*mariae* ammonite zone, *scarburgense* ammonite subzone) characterized by a sharp decrease upwards in illite and kaolinite balanced by an increase in smectitic minerals;

2 the occurrence of at least one smectite-dominated clay band located close to the Lower Oxfordian/Middle Oxfordian boundary (*cordatum*/*plicatilis* zones).

The mineralogical evolution may reflect a major palaeogeographic change (first connection between the Atlantic Ocean and the Paris Basin, or a change in detrital source areas) occurring in the *mariae* zone related to a second-order maximum flooding event superimposed on a possible climatic change from humid to arid conditions (Dugué, 1991; Pellenard *et al.*, 1999). Identification of primary volcanic crystals such as zircon, apatite and biotite indicates that the smectite-rich band has a volcanic origin and is therefore a bentonite (Pellenard *et al.*, 1999). Several questions arise from this interpretation. What is the geographical extension of the layer? Are there other bentonites intercalated in the succession? Is it possible to establish long-distance correlations in the Oxfordian using bentonites? What type of volcanism provides the source of the bentonite, and where were the volcanic active centres located?

In order to answer these questions, new investigations of Oxfordian outcrops in the Paris and Subalpine Basins were carried out. In the Paris Basin, a bentonite layer was found in an outcrop close to St Blin about 20 km to the south of ANDRA borehole HTM 102 (Fig. 1A). In the Subalpine Basin, 400 km to the south, coeval clay deposits correspond to the 'Terres Noires' Formation. Several representative sections have been studied throughout the basin in the search for bentonite layers (Fig. 1B). As shown below, volcanic clays were found in 10 sections. The

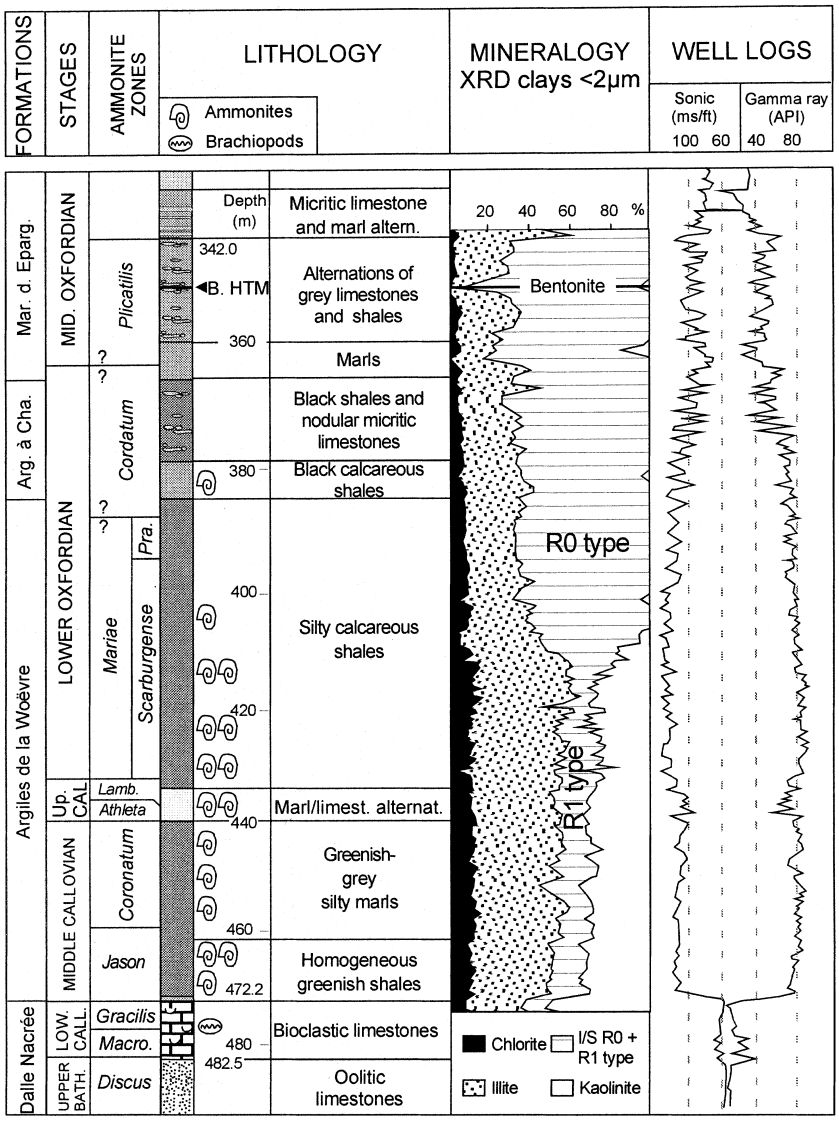

Fig. 2. Lithology, biostratigraphy, well logs and clay mineralogy of ANDRA borehole HTM 102 (Paris Basin). Logging data are from ANDRA. Arg. à Cha., Argiles à Chailles Formation; Mar. d. Eparg., Marnes des Eparges Formation; *Macro.*, *macrocephalus* zone; *Lamb.*, *lamberti* zone; *Pra.*, *praecordatum* zone; I/S, illite–smectite mixed layer.

bentonites occur at similar stratigraphic levels in both basins, so it is important to characterize and attempt to correlate these volcanic deposits in order to test their potential as long-distance isochronous markers. Thus, the objectives of this study were to characterize each bentonite layer through mineralogical and geochemical investigations and to establish correlations between the Paris Basin and the Subalpine Basin. In addition, geodynamic implications of the study will be examined.

METHODS

Detailed sedimentological logs were obtained throughout the Oxfordian silty clay formations in the two study areas. Smear slides, polished thin sections cut perpendicular to bedding, heavy mineral studies following heavy liquid separation and X-ray diffraction (XRD) analysis were used to characterize the mineral phases in the bentonite layers. Clay mineral associations were studied using XRD on oriented mounts. Deflocculation of clays was done by successive washing with distilled water after decarbonation of the crushed rock with 0·2 M HCl. The <2 μm clay fraction was separated by sedimentation and centrifugation. X-ray diffractograms were obtained using a Philips PW 1730 diffractometer with CuKα radiation and Ni filter. A tube voltage of 40 kV and a tube current of 25 mA were used. Three X-ray scans were performed, after air drying, ethylene glycol solvation and heating at 490 °C for 2 h. The goniometer was scanned from 2·5° to 28·5° 2θ for air-dried and glycol-solvated samples, and from

2·5° to 14·5° 2θ for heated samples. The identification of clay minerals was made according to the position of the (001) series of basal reflections on the three X-ray diffractograms and followed international nomenclature (Brown & Brindley, 1980; Reynolds, 1980; Moore & Reynolds, 1997). Semi-quantitative analyses were obtained from the area of the (001) series of mineral basal reflections on the ethylene glycol solvation trace using MACDIFF 4.1.2 software written by Petschick (2000). Differential thermal analyses of the clay fraction were obtained using a SETARAM Tag 24 simultaneous symmetrical thermoanalyser. Geochemical data were obtained using the inductively coupled plasma (ICP) techniques after $LiBO_2$ and HNO_3 digestion (Nancy CRPG Laboratory). Major elements were analysed by ICP-AES and trace elements by ICP-MS. Ten major and 43 trace elements were determined in whole-rock samples of both bentonites and associated shales.

IDENTIFICATION OF BENTONITES

Field and borehole identification

Eastern Paris Basin

Oxfordian sediments from the Paris Basin have been studied for many years (Debrand-Passard *et al.*, 1980; Dugué, 1991; Lefrançois *et al.*, 1996), but volcanogenic deposits have not been recognized previously. This probably reflects the difficulty in identifying individual millimetre-thick to centimetre-thick clay bands intercalated in a thick homogeneous clay-rich formation. In the eastern part of the Paris Basin, the Callovian–Oxfordian deposits, including the Argiles de la Woëvre, Argiles à Chailles and Marnes des Eparges Formations, consist of 130 m of clays and silty clays with occasional carbonate beds that occur mainly in the topmost part (Fig. 2). The first identification of a bentonite was in ANDRA borehole HTM 102: XRD analyses of the clay fraction in closely spaced samples (one sample every 50 cm) revealed the occurrence of a single smectite-dominated horizon (bentonite Htm, sample Htm102) within illite–smectite-rich (I/S) enclosing clays and marls (Fig. 2; Table 1). In the core, this clay band, located at 351·42 m depth, is visually almost indistinguishable from the enclosing shales (Fig. 3A). Only rare ammonites were found near the bentonite, which probably occurs close to the boundary between Lower and Middle Oxfordian (Pellenard *et al.*, 1999). The same layer Htm was identified in two other boreholes, ANDRA EST 103 (sample Est103) and ANDRA EST 104 (sample Est104), located 3 km to the north (Fig. 1, Table 1), and these were correlated with borehole HTM 102 using well logs together with biostratigraphic evidence (ANDRA, 2000; Fig. 2). Only poor outcrops are available in this area, the above-mentioned formations being largely covered by vegetation. However, near St Blin, 20 km to the south, a succession of Lower/Middle Oxfordian mudrocks also contains a greyish band (Fig. 3B and C) with a smectite-dominated clay fraction suggesting a volcanic origin and a possible correlation with the bentonite of boreholes HTM 102, EST 103 and EST 104. In the field, the bentonite horizon is distinguished by its lighter colour and, as water is preferentially absorbed by smectite, the bentonite is typically wetter and more plastic than the enclosing clays.

Subalpine Basin

The Callovian–Oxfordian deposits of the Subalpine Basin correspond to the Terres Noires Formation (Artru, 1972) and consist of several hundred metres of clays, silty clays and marls with common nodular rusty or buff-coloured carbonate beds (Fig. 4), which accumulated from the Bathonian to the Oxfordian in a rapidly subsiding basin (Debrand-Passard *et al.*, 1984). This basin was surrounded by carbonate platforms and by extensional or strike-slip fault systems, inherited from Tethyan rifting (Lemoine & de Graciansky, 1988; de Graciansky *et al.*, 1999). A dominance of distal offshore depositional environments and high sedimentation rates (100 m Myr^{-1} on average) make the Terres Noires Formation particularly suitable for the preservation of volcanic ash falls.

Detailed sedimentological logs were constructed for the Lower/Middle Oxfordian interval (Fig. 4). Several clay layers, 1–10 cm in thickness and laterally continuous (Fig. 5A) were considered as probable bentonites because of their pale colour (pale grey, ochre to orange; Fig. 5B–D) and because they are softer and more plastic than the enclosing marls, as observed for most bentonite deposits elsewhere (Teale & Spears, 1986; Merriman & Roberts, 1990; Kolata *et al.*, 1996; Spears *et al.*, 1999; Jeans *et al.*, 2000). In addition, these clay layers are picked out by vegetation because the smectite sheets absorb more water than other clay minerals and provide an environment that encourages more abundant plant growth (Fig. 5D). Five horizons were positively identified as bentonites in the Terres Noires Formation.

Table 1. Main characteristics and locations of the studied samples.

Location	Sample	Borehole depth (m)	Type	Location	Ammonite zone; subzone	Bentonite thickness (cm)	Mineralization thickness (cm)
Paris Basin	Htm 102	351·42	Bentonite Htm	ANDRA HTM102 borehole	*plicatilis* (?)	12	NA
	Est 103	429·40	Bentonite Htm	ANDRA EST 103 borehole	*plicatilis* (?)	10	NA
	Est 104	429·05	Bentonite Htm	ANDRA EST 104 borehole	*plicatilis* (?)	12	NA
	Sb 16	NA	Bentonite Sb16	St Blin	*plicatilis* (?)	12	NA
	Sh. Sb 11	NA	Shale St Blin	St Blin	*plicatilis*; *vertebrale*	NA	NA
	Sh. Sb 21	NA	Shale St Blin	St Blin	*cordatum*; *costicardia*	NA	NA
Subalpine Basin	B1 Oze	NA	Bentonite B1	Oze	*cordatum*	<1	NA
	B2 Oze	NA	Bentonite B2	Oze	*cordatum*/*plicatilis*	<1	NA
	B3 Oze	NA	Bentonite B3	Oze	*plicatilis*; *vertebrale*	<1	NA
	B5 Oze	NA	Bentonite B5	Oze	*plicatilis*; *antecedens*	<1	NA
	Mbo Oze	NA	Bentonite Mbo	Oze	*plicatilis*; *vertebrale*	10–15	4
	Mbo Oze2	NA	Bentonite Mbo	Oze	*plicatilis*; *vertebrale*	10–15	4
	Mbo Mls	NA	Bentonite Mbo	Montréal-les-Sources	*plicatilis*; *vertebrale*	2	1–2
	Mbo Bar	NA	Bentonite Mbo	Barsac	*plicatilis*; *vertebrale*	3	NA
	Mbo Bar2	NA	Bentonite Mbo	Barsac	*plicatilis*; *vertebrale*	3	NA
	Mbo Bea	NA	Bentonite Mbo	Beauvoisin	*plicatilis*; *vertebrale*	2	0–3
	Mbo Bui	NA	Bentonite Mbo	Buis-les-Baronnies	*plicatilis*; *vertebrale*	1–2	0–1
	Mbo Rib	NA	Bentonite Mbo	Ribiers	*plicatilis*; *vertebrale*	2	0–1
	Mbo Rib2	NA	Bentonite Mbo	Ribiers	*plicatilis*; *vertebrale*	2	0–1
	Mbo Sia	NA	Bentonite Mbo	Les Sias	*plicatilis*; *vertebrale*	8–10	0–1
	Sh. Oze 97A	NA	Shale	Oze	*plicatilis*; *vertebrale*	NA	NA
	Sh. Oze 141	NA	Shale	Oze	*plicatilis*; *antecedens*	NA	NA
	Sh. Mls 64	NA	Shale	Montréal-les-Sources	*plicatilis*; *vertebrale*	NA	NA

NA, not applicable.

© 2003 International Association of Sedimentologists, *Sedimentology*, **50**, 1035–1060

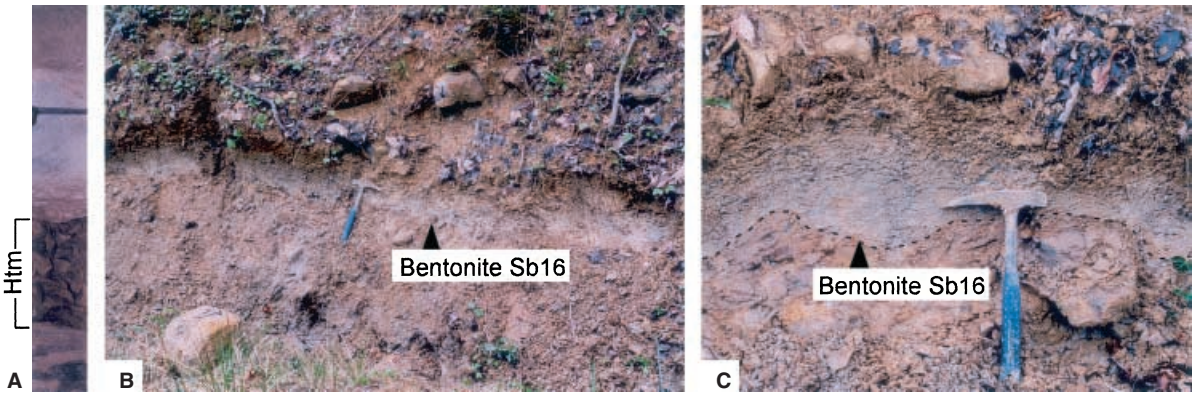

Fig. 3. Bentonite layers sampled from the Paris Basin. (A) Bentonite Htm (12 cm) occurring in the ANDRA borehole HTM 102. (B and C) St Blin outcrop showing a 12 cm thick bentonite layer (Sb16). The hammer shaft is 30 cm long.

Four of them correspond to millimetre-thick clayey horizons (B1, B2, B3, B5 Oze), while the fifth corresponds to a thicker bed, commonly associated with sulphate/carbonate mineralization, named here 'the mineralized bentonite of Oze' (Mbo; Fig. 5C and D; Table 1). This distinctive bentonite was identified in 10 sections, and constitutes an excellent marker bed throughout the Subalpine Basin where it can easily be correlated from section to section (Fig. 4). These layers are well-constrained biostratigraphically based on ammonites (Fortwengler, 1989; Marchand *et al.*, 1990; de Graciansky *et al.*, 1999). The stratigraphic positions are as follows (Fig. 4; Table 1): B1, top of *cordatum* zone (Lower Oxfordian); B2, *cordatum/plicatilis* boundary (Lower Oxfordian/Middle Oxfordian boundary); B3, base of *vertebrale* subzone of the *plicatilis* zone (Middle Oxfordian); Mbo, *vertebrale* subzone of the *plicatilis* zone; B5, *antecedens* subzone of the *plicatilis* zone.

Mineralization associated with bentonite deposits

Descriptions of secondary mineralization associated with bentonite deposits are scarce. Some bentonites show calcareous concretions, veins of silica subparallel to the bedding or layers of chert underlying thicker beds (Merriman & Roberts, 1990; Kolata *et al.*, 1996). In some places, mineralization occurs at the base of the bentonite. Of the 10 studied sections, six of them show the bentonite systematically associated with a mineralized zone of variable composition and thickness (Table 1). This zone is typically composed of sulphate/carbonate concretions or thin discontinuous veins. Minerals identified by optical microscopy and XRD include fibrous crystals of calcite, celestite and barite, growing perpendicular to bedding. Associated deformation (compaction) in microstructures suggests an early formation but, in places, neoformed authigenic crystals of barite indicate secondary recrystallization.

Bentonite petrography

Bentonites from the Paris Basin contain uncommon glass shards that are recognizable in thin sections, under the binocular microscope or under a scanning electron microscope (SEM), but most of these shards are thought to have been replaced by clay minerals. Potassium feldspars including sanidine and microcline have been identified by SEM and petrographic microscope. Euhedral crystals of zircon, apatite and biotite are identified in smear slides and thin sections (Fig. 6), but these correspond to only a minor component of the bulk rock which is dominantly composed of clay minerals. Other minerals include quartz, calcite, dolomite and phosphate grains, with minor muscovite, pyrite and accessory abraded zircon. Authigenic kaolinite or leverrierite crystals with a vermiform habit have been identified in the fraction coarser than 10 μm. Rare bioclasts (bivalve, echinoderm or brachiopod) are also preserved in these deposits. Thin-section and SEM observations reveal a matrix composed dominantly of folded lamellar smectite

Fig. 4. Detailed logs and correlation of some measured sections from the Subalpine Basin showing the thick bentonite Mbo and the millimetre- to centimetre-thick bentonites B1, B2, B3 and B5. Correlations are based on key marker beds, lithological units, bentonites and biostratigraphic data. *T*, *transversarium* zone; *Buk.*, *bukowski* subzone; *Prae.*, *praecordatum* subzone.

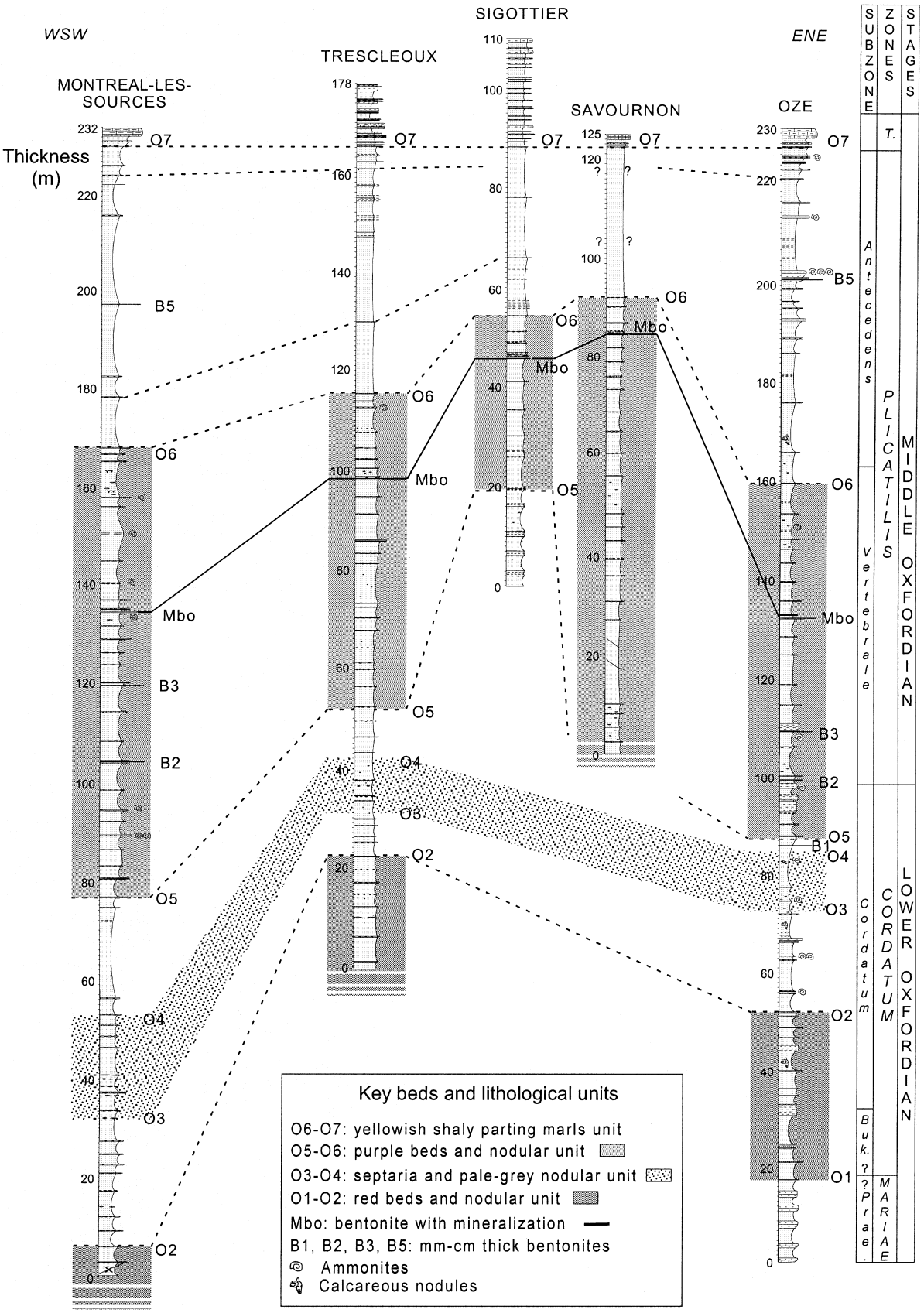
WSW
MONTREAL-LES-SOURCES
TRESCLEOUX
SIGOTTIER
SAVOURNON
OZE
ENE
Thickness (m)
SUBZONE
ZONES
STAGES
T.
Antecedens
PLICATILIS
MIDDLE OXFORDIAN
Vertebrale
Cordatum
CORDATUM
LOWER OXFORDIAN
Buk.
?Prae.
MARIAE
O7
O6
O5
O4
O3
O2
O1
Mbo
B5
B3
B2
B1
Key beds and lithological units
O6-O7: yellowish shaly parting marls unit
O5-O6: purple beds and nodular unit
O3-O4: septaria and pale-grey nodular unit
O1-O2: red beds and nodular unit
Mbo: bentonite with mineralization
B1, B2, B3, B5: mm-cm thick bentonites
Ammonites
Calcareous nodules

Fig. 5. Field photographs of bentonites occurring in the Terres Noires Formation of the Subalpine Basin. (A) Bentonite B1 at Oze. (B) Bentonite B3 at Oze showing a typical ochre alteration; pen is 15 cm long. (C) Bentonite Mbo at Oze with associated sulphate mineralization. (D) Bentonite Mbo at Beauvoisin; hammer shaft is 30 cm long.

aggregates, showing a flexural texture (Fig. 6D). X-ray powder diffraction analyses carried out on both bulk rock and the <2 μm fraction reveal lower quartz (Fig. 7) and calcium carbonate contents than in the enclosing claystones (confirmed by lower SiO_2/Al_2O_3 ratio and CaO content; Table 3) and more alkali feldspar. Detrital grains of quartz, potassium feldspar (orthoclase, microcline), muscovite and abraded zircon are common in the enclosing shales. These minerals are also identified in the bentonite deposits, suggesting possible detrital contamination during or after ash deposition. Calcite, ferroan dolomite and framboidal pyrite are common diagenetic minerals, and typically form by precipitation during early and late diagenesis. Bentonites of the Subalpine Basin occasionally contain abundant sulphates (barite, celestite) derived from the underlying mineralization. Jarosite and pyrite are occasionally identified in some samples by microscopy or XRD (Table 2).

Mineralogy of the clay fraction

Paris Basin bentonites

Samples of bentonite from the ANDRA boreholes and from the St Blin section are composed dominantly (95%) of a random illite–smectite mixed layer (I/S R0; Table 2, Fig. 7A). Using the saddle/001 ratio method (Inoue *et al.*, 1989) to

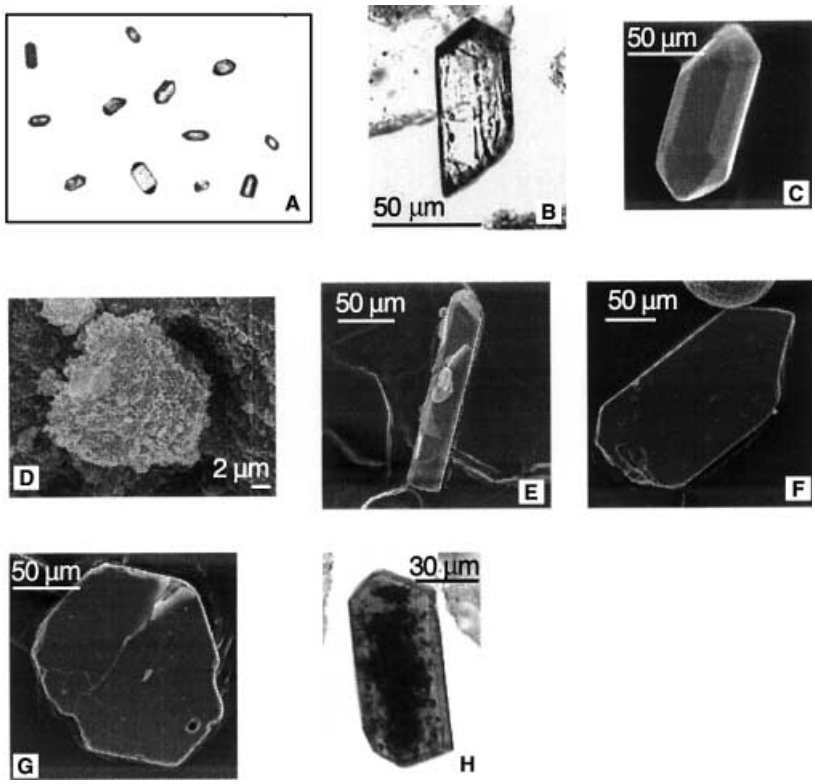

Fig. 6. Smear slide photomicrographs and SEM photographs of: (A–C) euhedral and subeuhedral zircons, (D) folded lamellar smectite aggregates from bentonite Htm, (E and F) apatite crystals, (G) biotite, (H) amphibole.

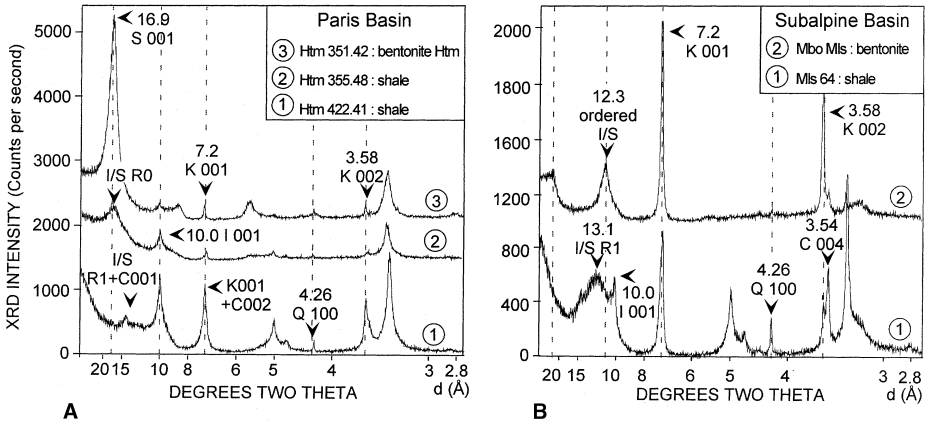

Fig. 7. (A) Comparison between X-ray diffraction (XRD) traces (clay fraction <2 μm) of bentonite Htm and detrital shales from ANDRA borehole HTM 102. (1) Illite- and kaolinite-dominated clay assemblage from the lower part of the borehole (*scarburgense* subzone), (2) illite–smectite mixed layer and illite-dominated clay assemblage from the upper part of the borehole (*plicatilis* zone), (3) smectite-dominated clay assemblage from bentonite Htm. (B) Comparison between XRD traces (clay fraction <2 μm) of bentonite Mbo and detrital shales from Montréal-les-Sources (Subalpine Basin). (1) Typical detrital assemblage including illite, kaolinite, chlorite and random I/S mixed layer R1, (2) mixture of ordered illite–smectite mixed layer and authigenic kaolinite from bentonite Mbo. C, chlorite; I, illite; I/S, illite–smectite mixed layer; K, kaolinite; Q, quartz; S, smectite.

estimate the percentage of smectite layers in I/S, the composition ranges from 75% to 95% of the smectite layer. These illite/smectite minerals show a (001) peak between 16·9 and 17·2 Å and a (060) reflection at 1·500 Å, indicating a dioctahedral character. Only minor phyllosilicates including kaolinite, chlorite, mica and probably other illite/smectite mixed-layer phases (R1) occur. In contrast, the clay fraction from the enclosing silty clays is very different (Fig. 7A). On average, this includes 30% illite, 70% mixed-layer I/S R0 containing 50–75% of smectite

Table 2. Mineralogy of bentonites from the Paris and Subalpine Basins.

Location	Sample	Kaolinite (%)	I/S (%)	Chlorite (%)	Illite (%)	I/S d(Å)	IS type	S in I/S (%)	Feldspar	Quartz	Pyrite	Jarosite
Paris Basin	Htm	2	95	1	2	16·96	R0	75–95	+	++	BD	BD
	Sb16	2	95	1	2	17·22	R0	80–97	+	++	BD	BD
Subalpine Basin	Mbo Bar	40	46	14	BD	13·30	reg. R1	ND	+	+	BD	BD
	Mbo Bar2	55	27	15	3	13·41	reg. R1	ND	+	+	BD	BD
	Mbo Bea	54	37	9	BD	13·61	ran. R1	ND	++	+	++	+
	Mbo Bui	43	37	10	10	13·45	reg. R1	ND	++	+	BD	BD
	Mbo Mls	48	35	10	8	12·33	reg. R1	ND	+	++	+	BD
	Mbo Oze	48	39	11	1	13·45	reg. R1	ND	BD	+	BD	BD
	Mbo Oze2	32	57	9	2	13·45	reg. R1	ND	+	++	BD	BD
	Mbo Rib	79	9	12	BD	12·98	ran. R1	ND	++	+	BD	BD
	Mbo Rib2	40	52	8	1	16·76	reg. R0	65–85	++	+	BD	BD
	Mbo Sia	56	23	19	2	13·78	reg. R1	ND	++	++	BD	BD

I/S, illite–smectite mixed layer; I/S d(Å), mixed-layer main reflection; reg. R1, regular R1-type I/S mixed layer; ran. R1, random R1-type I/S mixed layer; Feld., feldspar; +, occurrence; ++, abundant; BD, below detection; ND, not determined.

layers, and 5% chlorite. These clay mineral assemblages, which are common in most Upper Jurassic shales from the Paris Basin, are probably of detrital origin. They originated from the erosion of emerged land areas such as the London–Brabant Massif, Armorican Massif, perhaps the French Central Massif and from the North Atlantic Ocean margins (Dugué, 1991; Debrabant *et al.*, 1992; Pellenard *et al.*, 1999).

Differential thermal analysis (DTA) was carried out on most samples of bentonites. The curves show two characteristic endotherms at 500 °C and 650 °C (Fig. 8), suggesting a mixture of two distinct types of smectitic minerals (Deconinck & Chamley, 1995), including Cheto-type smectite formed by submarine weathering of volcanic glass shards and common detrital I/S mixed layers. Bioturbation (evidenced by the occurrence of burrows and a relatively low rate of deposition of the ash) or current effects may be responsible for this mixture, and may explain the presence of small amounts of detrital clays such as illite or chlorite as well as detrital quartz and feldspar grains. Kaolinite also occurs in the bentonite deposits. This mineral is commonly associated with smectite minerals in altered ash beds, mainly in continental settings; however, some authors have described kaolinite associated with smectite in ash layers deposited in marine environments (Teale & Spears, 1986; Spears *et al.*, 1999; Deconinck *et al.*, 2000).

Subalpine Basin bentonites

In the Subalpine Basin, the enclosing silty clay consists of a mixture of illite (45%), chlorite (20%), kaolinite (5%), R1-type mixed-layer I/S (30%) and abundant quartz (Fig. 7B). The clay assemblages of beds B1, B2, B3, B5 and Mbo show high proportions of smectitic minerals and kaolinite and differ significantly from the clay fraction of the enclosing silty clay (Fig. 7B). Ten samples of the thick bentonite (Mbo) originating from seven sections were studied (Table 2): Barsac (Mbo Bar, Mbo Bar2); Beauvoisin (Mbo Bea); Buis-les-Baronnies (Mbo Bui); Montréal-les-Sources (Mbo Mls); Oze (Mbo Oze, Mbo Oze2); Ribiers (Mbo Rib, Mbo Rib2); Les Sias (Mbo Sia; Fig. 1B). X-ray diffraction analysis performed on the <2 μm fraction of the bentonite bed reveals some clay mineralogical variability at both outcrop and basin scale (Table 2; Fig. 9). Kaolinite and mixed-layer illite/smectite regular or random R1 and R0 type are the dominant clay minerals with traces of chlorite and mica (Table 2, Fig. 7B). Average abundances calculated after estimation of diffraction peak heights and areas indicate 50% kaolinite, 35% I/S mixed layer, 10% chlorite and 5% mica.

One sample (Mbo Rib) is particularly rich in kaolinite (80%), and three samples show more I/S mixed layer than kaolinite. Kaolinite-dominated volcanic clay deposits are generally called tonsteins (Bohor & Triplehorn, 1993), but this typically refers to thin claystone beds in Carboniferous Coal Measures with a volcanic origin, so here the term of 'kaolinite-bentonite' is preferred, as proposed by Fisher & Schmincke (1984). Both regular and random mixed-layer I/S R1 type with a basal reflection around 13 Å were observed (Table 2). Mbo Rib2 presents an exception with a basal reflection at 16·7 Å; the saddle/001 ratio method indicates 65–85% of smectitic layer for

Table 3. Major, trace element and REE analyses of the studied samples.

	Bentonites and associated shales from the Paris Basin						Bentonites and associated shales from the Subalpine Basin								
	Htm 102	Est 103	Est 104	Sb 16	Sh. Sb 11	Sh. Sb 21	B1 Oze	B2 Oze	B3 Oze	B5 Oze	Mbo Oze	Mbo Mls	Mbo Bea	Sh. Oze 97A	Sh. Oze 141
Major elements (wt %)															
SiO_2	46·91	47·83	49·60	49·65	56·13	41·99	61·65	20·49	40·50	56·60	36·99	47·96	40·48	43·75	43·19
Al_2O_3	10·16	11·72	12·67	16·06	6·57	7·72	13·40	9·86	11·93	12·50	24·87	29·01	25·93	10·10	8·03
Fe_2O_3	2·98	2·53	2·28	2·91	2·43	3·01	6·77	6·43	5·55	5·17	2·36	4·52	5·68	4·29	3·33
MnO	<0·03	<0·03	<0·03	<0·03	<0·03	<0·03	0·09	0·17	0·11	0·02	0·05	<0·03	<0·03	0·02	0·01
MgO	2·59	2·60	2·67	1·64	0·84	1·18	1·37	1·36	1·29	1·38	1·13	0·43	0·40	1·33	1·21
CaO	14·81	11·59	9·71	7·65	15·10	21·57	3·63	30·37	16·76	7·90	6·32	0·61	3·86	18·70	21·45
Na_2O	0·26	0·31	0·33	0·08	0·05	0·05	0·43	0·21	0·28	0·46	0·21	0·78	0·97	0·35	0·31
K_2O	2·58	2·51	2·53	2·56	2·14	1·84	2·22	1·34	1·94	2·11	1·35	1·21	0·89	1·67	1·36
TiO_2	0·87	1·08	1·21	1·43	0·46	0·46	0·72	2·02	0·65	0·68	2·12	2·84	2·51	0·56	0·45
P_2O_5	0·18	0·24	0·23	0·21	<0·05	<0·05	0·08	1·72	0·06	0·16	0·50	0·25	0·42	0·06	0·08
SiO_2/Al_2O_3	4·61	4·08	3·91	3·09	8·54	5·43	4·60	2·07	3·39	4·53	1·48	1·65	1·56	4·33	5·37
Trace elements (p.p.m.)															
As	9·9	10·8	8·3	6·2	8·5	10·0	8·5	39·5	7·7	8·9	9·0	29·2	25·2	5·2	9·6
Ba	142	156	172	185	121	122	3410	1650	204	5650	7980	1090	1160	103	208
Be	0·47	1·23	<1	1·4	<1	1·43	1·39	1·22	1·98	1·49	<1	1·34	<1	1·73	0·89
Bi	0·08	0·10	0·11	0·10	0·10	0·14	0·18	0·05	0·15	0·18	0·11	0·23	0·16	0·15	0·11
Cd	0·62	<0·3	<0·3	0·31	<0·3	<0·3	0·07	0·42	0·33	0·15	2·00	<0·3	<0·3	0·14	0·22
Co	8·2	8·6	8·6	6·7	3·9	8·5	21·7	166	14·5	14·1	11·8	5·9	14·5	9·6	8·8
Cr	54·1	50·0	46·7	49·1	77·3	70·7	93·6	23·3	95·0	99·4	33·7	50·0	40·1	73·3	67·7
Cs	1·9	2·8	2·6	2·9	4·7	6·5	13·1	2·9	15·3	15·3	5·8	4·9	5·2	6·9	6·6
Cu	12·7	12·7	13·1	12·7	7·9	10·8	38·1	49·7	30·4	26·6	19·7	38·7	18·8	23·8	20·0
Ga	11·0	11·5	12·1	16·6	8·7	10·2	16·3	11·0	17·2	16·9	14·5	13·5	9·1	12·3	11·4
Ge	1·26	1·38	1·31	1·26	1·44	1·42	2·05	1·29	2·43	4·86	1·98	2·39	1·54	1·14	1·13
Hf	4·7	6·4	6·9	7·4	4·7	3·5	4·3	3·1	3·9	3·8	7·6	9·8	7·6	3·3	2·8
In	0·02	<0·01	<0·01	<0·01	<0·01	<0·01	0·06	0·08	0·05	0·06	<0·01	<0·01	<0·01	0·03	0·04
Mo	0·58	0·55	0·54	0·94	1·29	0·72	0·69	8·58	0·87	0·57	4·00	3·29	6·69	0·43	0·32
Nb	66·0	86·5	97·4	130	14·1	15·4	17·1	276	18·9	18·3	211	254	222	12·3	12·6
Ni	38·6	31·4	28·4	20·4	20·0	16·0	86·4	246	70·8	66·9	32·7	47·7	44·9	50·7	47·7
Pb	16·3	14·4	15·5	20·7	9·3	7·9	16·7	85·5	16·1	13·9	22·5	103	54·3	12·3	9·9
Rb	56·2	54·6	50·2	49·5	62·3	80·8	107	50·9	106	109	45·4	43·5	29·4	76·4	66·9
Sb	0·40	0·39	0·39	0·32	0·31	0·38	0·60	2·74	0·63	0·61	0·43	1·13	2·08	0·37	0·37
Sn	1·21	1·32	1·52	1·78	1·17	1·63	1·97	1·02	1·81	1·86	2·27	3·25	2·36	1·33	1·26
Sr	500	474	458	151	183	251	626	1230	576	479	31500	2730	1710	343	423
Ta	4·47	6·71	7·72	9·51	1·10	1·04	1·28	15·9	1·31	1·32	14·7	20·2	17·6	0·95	0·89
Th	10·8	13·9	14·8	16·3	7·0	6·5	11·5	23·3	11·5	10·8	24·5	32·3	24·9	8·7	7·5
U	1·78	3·30	3·94	3·24	1·44	1·81	2·03	7·51	1·72	1·84	4·64	6·95	7·90	1·47	1·21
V	83	92	92	117	66	88	116	333	118	134	148	169	157	80	93
W	1·02	1·34	1·33	1·63	1·05	1·24	1·80	2·87	1·57	1·62	1·64	2·89	2·76	1·21	1·02
Y	20·4	20·8	19·1	28·7	16·9	19·0	24·2	79·1	25·7	27·2	51·9	37·1	24·4	17·1	19·8
Zn	212	30	23	115	27	56	102	395	122	96	231	378	206	62	80
Zr	212	239	263	325	173	121	153	191	147	140	328	365	247	110	116
Rare earth elements (p.p.m.)															
La	32·8	34·0	33·0	69·3	23·4	26·6	31·5	222	33·5	32·7	124	145	107	25·0	24·4
Ce	65·6	68·6	65·7	138	35·3	41·3	64·4	420	64·1	57·7	271	319	232	41·4	41·5
Pr	8·40	8·60	8·50	15·7	4·80	5·20	6·65	41·5	7·10	6·75	29·6	30·0	21·2	4·90	5·10
Nd	31·1	33·9	32·7	54·4	16·7	21·0	26·4	152	27·1	25·7	107	95·7	67·1	18·1	18·2
Sm	5·18	5·84	5·89	8·93	3·28	3·79	5·77	28·2	5·26	5·58	19·0	13·0	8·72	3·56	3·44
Eu	1·25	1·48	1·41	2·36	0·74	0·81	1·87	7·13	1·14	1·98	3·75	2·85	2·03	0·69	0·76
Gd	3·77	4·62	4·70	6·6	2·84	3·16	4·81	24·9	4·36	4·69	14·0	7·64	5·36	2·91	3·03
Tb	0·56	0·66	0·62	0·98	0·42	0·47	0·71	2·93	0·61	0·68	1·91	1·20	0·79	0·46	0·41
Dy	2·98	3·41	3·30	5·37	2·49	2·74	4·07	14·5	3·60	3·94	9·59	6·77	4·50	2·54	2·60

Table 3. Continued.

	Bentonites and associated shales from the Paris Basin						Bentonites and associated shales from the Subalpine Basin								
	Htm 102	Est 103	Est 104	Sb 16	Sh. Sb 11	Sh. Sb 21	B1 Oze	B2 Oze	B3 Oze	B5 Oze	Mbo Oze	Mbo Mls	Mbo Bea	Sh. Oze 97A	Sh. Oze 141
Ho	0·60	0·68	0·63	0·93	0·49	0·58	0·80	2·29	0·69	0·75	4·64	1·20	0·84	0·53	0·53
Er	1·53	1·64	1·57	2·56	1·49	1·48	2·03	5·24	1·95	2·07	4·48	3·58	2·53	1·45	1·41
Tm	0·20	0·21	0·23	0·33	0·21	0·25	0·35	0·72	0·31	0·31	0·52	0·44	0·34	0·21	0·23
Yb	1·33	1·49	1·56	2·23	1·43	1·54	2·20	3·74	1·91	2·01	3·33	2·93	2·00	1·53	1·37
Lu	0·22	0·24	0·23	0·35	0·24	0·22	0·31	0·54	0·30	0·31	0·47	0·40	0·29	0·24	0·23
Sum REE	155·5	165·3	160	308·0	93·8	109·1	151·8	925·7	151·9	145·2	593·6	629·7	454·7	103·5	103·2

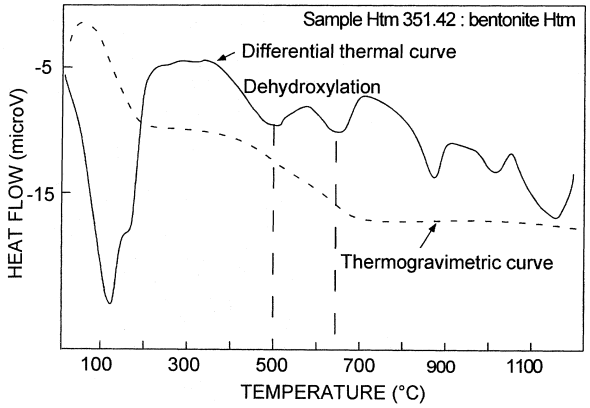

Fig. 8. Differential thermal curve (DTA) and thermogravimetric curve from bentonite Htm of the Paris Basin. The DTA curve shows two endotherms corresponding to dehydroxylation, indicating a mixture of two types of smectite.

this sample. The clay mineralogy of thin bentonites, B1, B2, B3 and B5, from Oze differs less from the enclosing shales. Kaolinite and I/S mixed layers are more abundant than in detrital deposits, but illite and chlorite occur in higher quantities than in the Mbo bentonite.

Geochemical data

Major element geochemistry

Early and late diagenetic processes may strongly modify the composition of bentonite layers (Fisher & Schmincke, 1984). Mobile elements are largely remobilized by the hydration responsible for the replacement of siliceous glass by clay minerals. Release of silica and the formation of clay minerals are commonly marked by lower values of SiO_2 and higher proportions of Al_2O_3 than in the enclosing claystones. The SiO_2/Al_2O_3 ratio reaches 3·5 in the bentonite samples from the Paris Basin and 5·5–8 in the enclosing rocks (Table 3). In the Subalpine Basin, this ratio is about 1·5–4·6 in the bentonite samples compared with 5·0 on average for the shales. These differences between the bentonites and the enclosing clays result from the occurrence of more detrital quartz grains in the shales than in the bentonites and the argillation of volcanic glass. SiO_2/Al_2O_3 ratios are generally lower in the Subalpine bentonites than in samples from the Paris Basin, probably because kaolinite is more abundant in bentonites from the Subalpine Basin than in bentonites from the Paris Basin.

Calcium values are generally lower in bentonite samples than in the associated mudrocks; Ba or Sr enrichment, which affects most bentonite samples from the Subalpine Basin, is probably related to fluid migration, which is known to have occurred in this basin (Gaidon, 1988; Guilhaumou *et al.*, 1996). Barium-, Sr- or Ca-rich fluids are preferentially trapped below bentonite horizons, which constitute a permeability barrier. This mechanism may be responsible for the mineralization occurring at the base of thick bentonite Mbo.

Surprisingly, K_2O contents are higher in the smectite-dominated bentonite samples from the Paris Basin than in those from the Subalpine Basin, which are characterized by the occurrence of I/S. This relationship may be explained by the more frequent K-feldspar grains occurring in the Paris Basin. The immobile oxide TiO_2 is generally more abundant in the bentonites, because of the occurrence of minerals such as rutile, and is a useful parameter in conjunction with the SiO_2/Al_2O_3 ratio for discriminating between volcanic vs. detrital influences (Fig. 10). High P_2O_5 contents in the bentonite samples compared with the enclosing shales probably reflects the occurrence of volcanogenic apatite crystals observed in SEM (Fig. 6E and F).

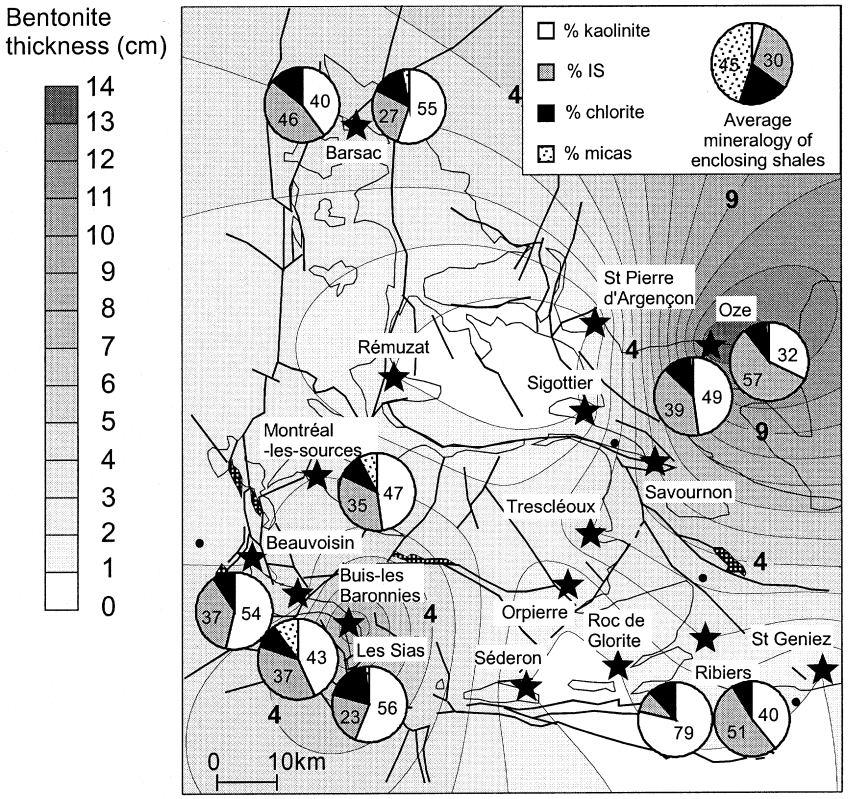

Fig. 9. Isopach map and clay mineralogy of bentonite layer Mbo in the Subalpine Basin.

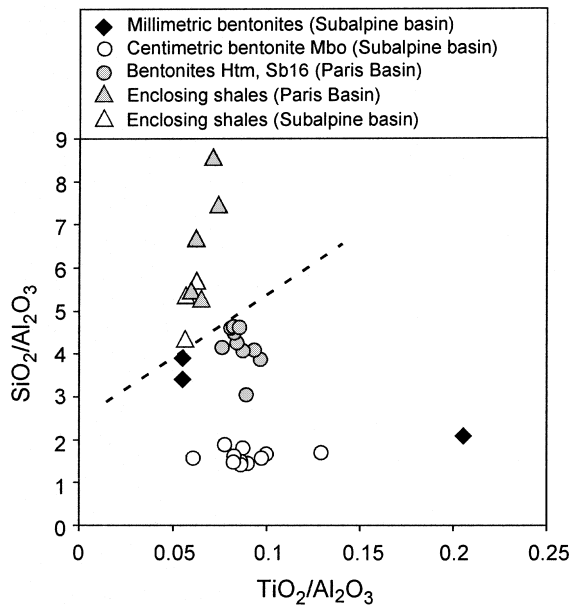

Fig. 10. TiO_2/Al_2O_3 vs. SiO_2/Al_2O_3 plot showing a discrimination between bentonite samples and detrital shales.

Trace element geochemistry

A comparison of the trace element profiles of five samples of shales from both basins (Table 1) shows a similar geochemical pattern (Fig. 11), whereas bentonite samples from both basins show positive and negative anomalies. Zirconium, Zn, Th, Y, Hf, U, Pb and, particularly, Nb and Ta are systematically and significantly enriched in the bentonite deposits compared with associated shales, whereas Cr, Rb and Cs are depleted (Table 3, Fig. 11). These geochemical features are frequently observed in bentonite samples and used for their discriminating power between detrital shales and volcanic products (Fisher & Schmincke, 1984; Pacey, 1984; Merriman & Roberts, 1990; Roberts & Merriman, 1990; Clayton *et al.*, 1996; Batchelor & Jeppsson, 1999; Spears *et al.*, 1999). This enrichment results partly from the original chemistry of the magma and from high concentrations in heavy minerals such as zircon $Zr[SiO_4]$, monazite (Ce, La, Th)PO_4, anatase TiO_2 and rutile TiO_2, as observed in smear slides or SEM. Some elements, including Ba, Sr, V, Ar, Co, Sb and Mo, are occasionally enriched in bentonite samples, notably those from the Subalpine Basin.

REE distribution

Chondrite-normalized rare earth elements (REE) or Cody shale-normalized REE (REE/SCo-1) patterns show that REE contents are higher in the

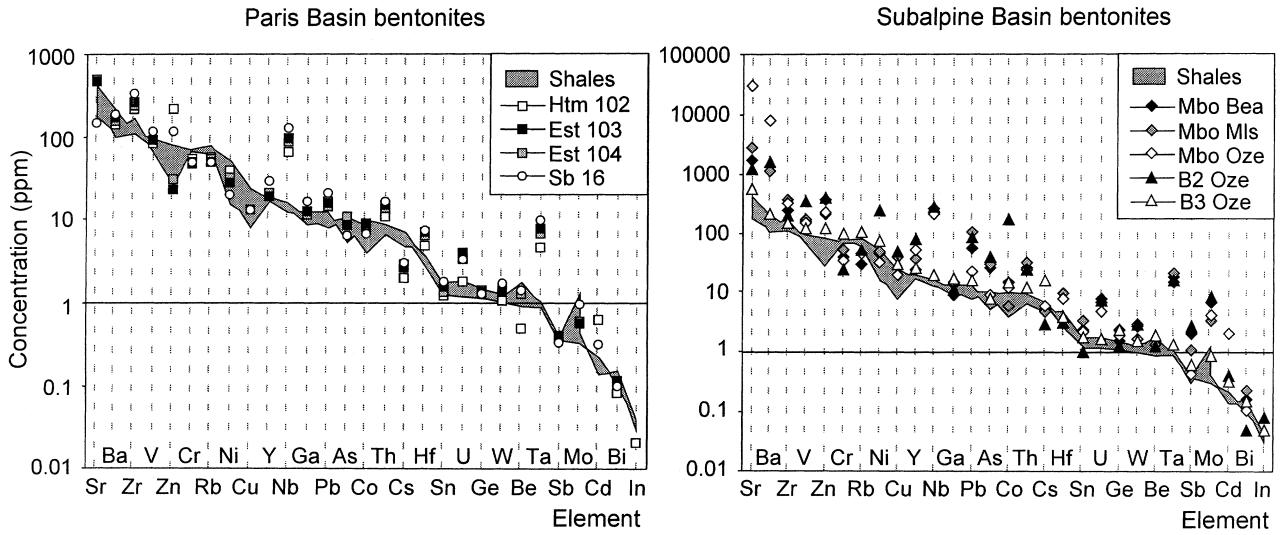

Fig. 11. Trace element concentrations (p.p.m.) of bentonites and associated shales from the Paris and the Subalpine basins.

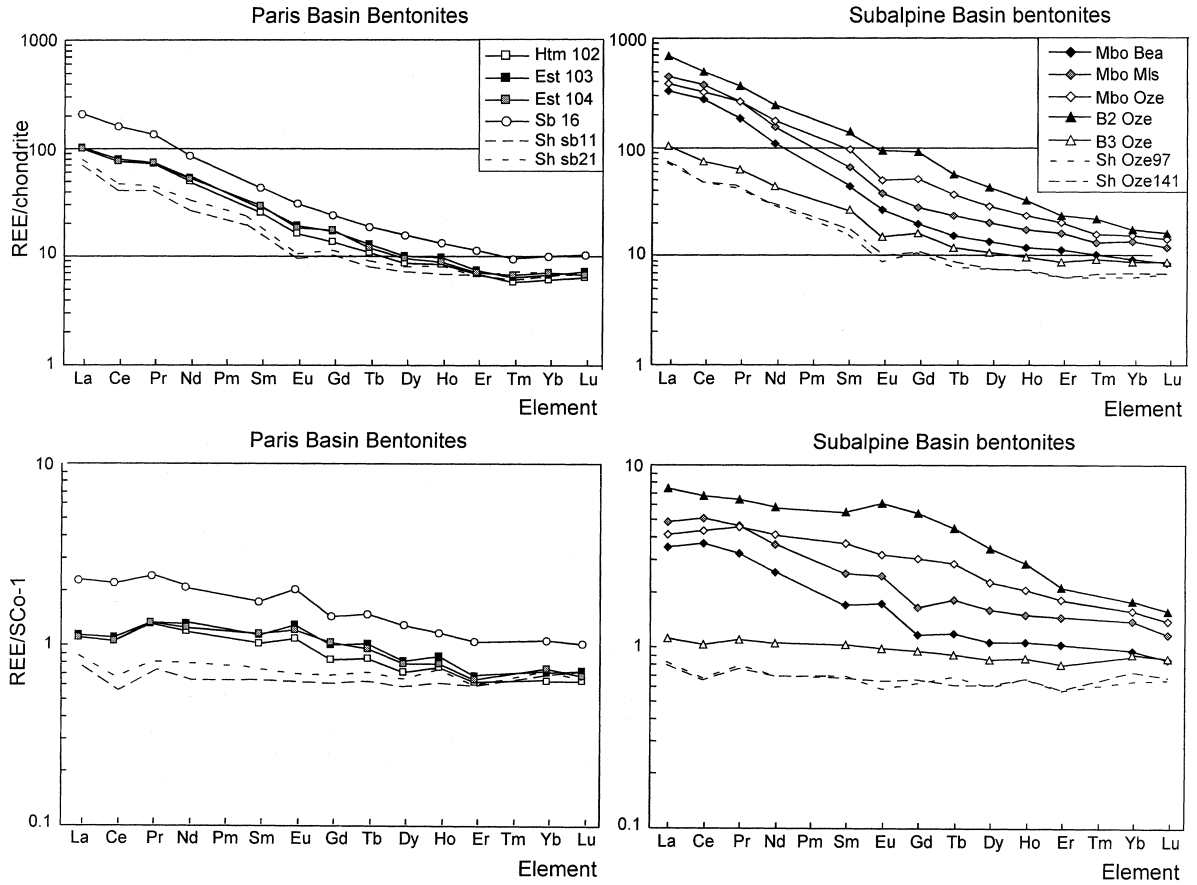

Fig. 12. Chondrite and Cody-shale-normalized REE plots of bentonites and associated shales from the Paris and Subalpine Basins. Chondrite values used for normalization from Evensen *et al.* (1978); SCo-1-values from Jarvis & Jarvis (1985).

bentonite samples than in the associated shales (Table 3), particularly for the light REE (LREE; Fig. 12). Slightly negative anomalies in Eu are generally observed for chondrite-normalized REE values of the Paris Basin and Subalpine bentonite samples, whereas shale samples are characterized

by more pronounced negative anomalies in Eu and Ce. Bentonites of the Paris Basin have a similar REE profile.

DISCUSSION

Correlation of bentonites from the Paris Basin

In the ANDRA boreholes and in the St Blin section, a bentonite layer occurs close to the Lower Oxfordian/Middle Oxfordian boundary (between the *cordatum* and *plicatilis* zones). In ANDRA borehole HTM 102, the bentonite layer Htm occurs at 351·42 m depth, while the occurrence of *Arisphinctes* sp. indicates the *plicatilis* zone (Middle Oxfordian) at 351·01 m depth, which is 40 cm above the bentonite. The determination of a *Campylites* or *Neoprionoceras* at 381·35 m indicates the *cordatum* subzone (Lower Oxfordian), but no biostratigraphical data are available between 351·01 and 381·35 m. Thus, bentonite Htm probably occurs in the *plicatilis* zone, but additional biostratigraphical data are needed to resolve this uncertainty (Fig. 2). This bentonite layer occurs at 429·40 m depth in ANDRA borehole EST103 and at 429·05 m depth in borehole EST104, but no additional biostratigraphical data are available for these. At St Blin, a bentonite (Sb16) is recorded in a 3 m thick interval without any ammonites, but this interval is between the *cordatum* subzone, the last subzone of the *cordatum* zone, and the *vertebrale* subzone, the first subzone of the *plicatilis* zone (Collin & Courville, 2000). Therefore, correlation of the bentonite layers in the three boreholes and Sb16 is consistent with the available biostratigraphic data.

The Paris Basin bentonites show common mineralogical features and similar geochemical fingerprints (Figs 11–13). Trace elements (Fig. 11) show similar patterns with small differences in Sr, Zn, U, Be and Cd, which may have been affected by early and late diagenetic processes. The bentonite from St Blin is characterized by an increase in total REE and some enrichment in the LREE. If this bentonite layer corresponds to the

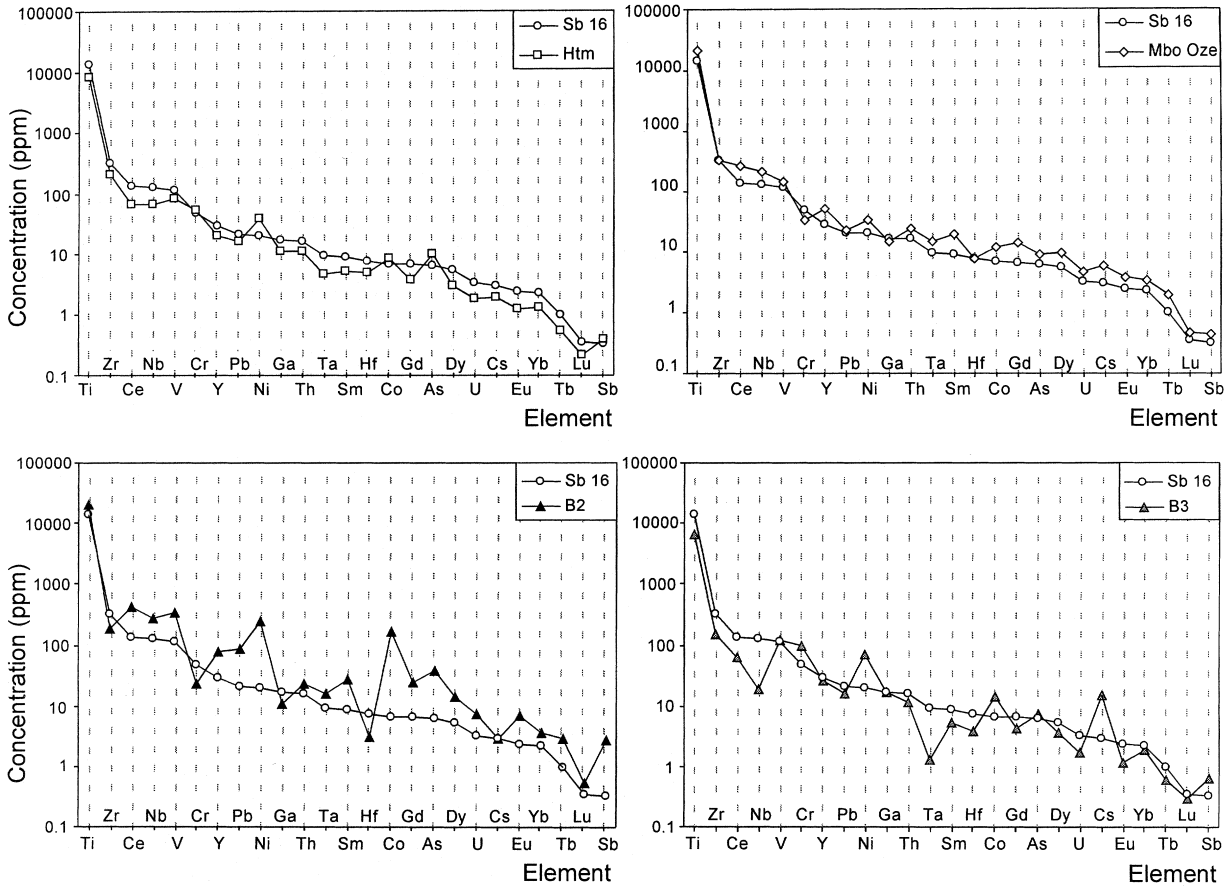

Fig. 13. Comparison of chemical fingerprints of bentonite samples from both basins.

same event as the bentonite in the boreholes, it may be less mixed with enclosing marls by bioturbation, and this may explain the increased REE content.

The common mineralogical features of the bentonite layers are not by themselves discriminant criteria that can be used reliably to correlate the different horizons, because bentonite layers commonly show a similar composition for their clay fraction (Wray, 1995, 1999). Therefore, a statistical analysis (see below), based on the chemical fingerprint of each layer, was conducted to evaluate the potential correlation between the ANDRA boreholes and the St Blin section.

Correlation of bentonites from the Subalpine Basin

In the Subalpine Basin, five distinct bentonites have been recognized. One bed, the Oze mineralized bentonite (Mbo), varies in thickness from 2 to 15 cm, and has been correlated between 10 sections covering 2000 km^2 (Fig. 9). Nevertheless, no evidence for any particular source direction is indicated by the isopach map (Fig. 9). Layer Mbo occurs in the *vertebrale* subzone (*plicatilis* zone, Middle Oxfordian) 34 m above the boundary between the Lower and Middle Oxfordian. This bentonite is much easier to correlate than those in the Paris Basin, because of the presence of a distinctive succession of purple variably nodular calcareous marker beds occurring above and below the bentonite (Fig. 4), and the occurrence of an abundant ammonite fauna. Correlation of bentonites B1, B2, B3 and B5 is more difficult as a result of their thin nature. An attempt was made to correlate these beds between Oze and the Montréal-les-Sources section, 40 km to the west (Fig. 4). Three millimetre thick beds were correlated (B2, B3, B5) based on to their positions relative to key lithostratigraphic marker beds, constrained by the available biostratigraphical data.

Clay mineral variation of the Mbo bentonite

Bentonites from the Subalpine Basin show abundant either random or regular R1 I/S and kaolinite, whereas the bentonites from the Paris Basin are dominantly composed of smectites (Table 2). Clay mineralogical analysis of the Mbo bentonite throughout the Subalpine Basin indicates great variability at both outcrop and basin scales. Samples Mbo Rib and Mbo Rib2 from the same outcrop (Ribiers) are characterized by the dominance of either kaolinite (80%) or I/S mixed layer (50%; Fig. 9, Table 1). At a basin scale, R1 I/S appears to be more regular (better crystallinity) in the north-east of the Subalpine Basin (Oze and Barsac sections), suggesting an increasing diagenetic influence towards the north-east. This is in agreement with diagenetic gradients in the basin indicated by clay mineral compositions and organic matter maturity (Deconinck & Debrabant, 1985; Deconinck, 1987; Levert *et al.*, 1988). R1 I/S probably originated by burial diagenetic replacement of smectites previously formed by syndepositional weathering of volcanic glass.

Bentonites from the Subalpine Basin are also characterized by the occurrence of abundant well-crystallized kaolinite. The distribution of the kaolinite within the bentonite layer is independent of the geographical location and seems also to be independent of the increasing burial diagenesis occurring towards the north-east of the basin (Fig. 9). Kaolinite-bentonites or tonsteins are usually characteristic of continental environments, but kaolinite-rich bentonites occur occasionally in open-marine sediments (Teale & Spears, 1986; Spears *et al.*, 1999; Deconinck *et al.*, 2000). However, it is difficult to explain the syndepositional replacement of volcanic glassy particles by kaolinite in marine waters (Spears *et al.*, 1999). The formation of kaolinite is favoured in acid, freshwater environments (Spears, 1970; Fisher & Schmincke, 1984; Spears *et al.*, 1999). According to fauna and microfauna and a boron content ranging from 295 to 490 $\mu g\ g^{-1}$ (Tribovillard, 1989), the Terres Noires Formation was deposited in open-marine normal or slightly hypersaline environments. Therefore, if we rule out the possibility of a period of low salinity in the basin, the origin of kaolinite could result either from the transformation of volcanic glass in acid microenvironments or the later fluid circulation that was probably responsible for the widespread mineralization at the base of the bentonite layer.

Chemical variation of the Mbo bentonite

Geochemical profiles for Mbo bentonite samples show minor differences mainly for SiO_2, Fe_2O_3, CaO, Ba, Sr, Co, Pb, Sb, As and REE, especially the middle REE (Figs 11 and 12; Table 3). Positive anomalies in Sr and Ba are easily explained by contamination from crystals of barite and celestite originating from the underlying mineralization. Variations in other elements may also result from sulphate precipitation in relation to fluid circulation, which occurred at different periods (Guilhaumou *et al.*, 1996). Samples Mbo Oze and Mbo Mls have higher REE concentrations than sample

Mbo Bea, but a similar REE pattern is observed with a constant ratio of LREE/HREE (Fig. 12), as indicated by similar La_N/Yb_N ratios. These differences might be produced by variable mixing with the enclosing sediment after deposition or variable conditions of argillization during early and late diagenesis, but the presence of significant sulphates in the analysed material may also contribute to the overall depletion of REEs in some samples.

Interbasin correlation of bentonites

Long-distance correlations of bentonites from the Paris to the Subalpine Basin are more speculative. Five bentonites have been identified in the Subalpine Basin while only one occurs in the Paris Basin. The mineralogy of the clay fractions of the bentonites from the two basins shows significant differences because of the diagenetic changes related to greater burial depth and fluid migration in the Subalpine Basin, so clay mineralogy cannot be used to correlate bentonite layers between the two areas. However, a comparison of the chemical fingerprints should help to correlate the Paris Basin bentonite with one of the Subalpine Basin bentonites (cf. Huff, 1983; Cullen-Lollis & Huff, 1986; Kolata *et al.*, 1987; Huff & Kolata, 1990). The geochemical data for each bentonite show common anomalies, but differences are apparent for elements with a high discriminator power such as Ti, Cr, Co, Ga, As, Zr, Sb, Cs, Ce, Sm, Eu, Tb, Dy, Yb, Lu, Hf, Ta, Th and U, as used previously by Cullen-Lollis & Huff (1986) and Kolata *et al.* (1987), or V, Ni, Y, Nb, Pb and Gd, which also show variations. These elements were used to compare the chemical fingerprints of the bentonite at St Blin with those in the ANDRA boreholes and in the Subalpine Basin. In the search for distinguishing chemical characteristics in the bentonites, it was assumed that the concentrations of those elements that are unique to each bed were similarly different in the separate ash falls. It has been shown in studies of Cenozoic tephras (Borchardt *et al.*, 1971; Randle *et al.*, 1971; Westgate *et al.*, 1977) that the immobile elements are useful in distinguishing between different ash beds. It was additionally assumed that the immobile element concentrations have been preserved or have been altered consistently in the transformation of volcanic ash to bentonite and, further, that the chemical composition of the original ash was constant over the region or varied systematically along a line from the source to the point of deposition.

Among the bentonites identified in the Subalpine Basin, B2 shows a chemical profile that is quite different from the Paris Basin bentonite (Fig. 13): Pb, Ni, Co, As and more immobile elements such as Nb, V, Y, U, Sb and REE are enriched, while Zr, Cr, Ga and Hf are depleted, suggesting that this deposit corresponds to a different volcanic event. Bentonites B1, B3 and B5 show similar chemical profiles. These beds are enriched in Ni, Co and Cs and depleted in Nb, Ce and Ta (Fig. 13) compared with Paris Basin bentonite Sb16, suggesting different events. In addition, according to the biostratigraphical data, B1 belongs to the *cordatum* ammonite subzone, and B5 belongs to the *antecedens* subzone, indicating that beds are older and younger, respectively, than the Paris Basin bentonite. Bentonites Mbo and Sb16 show very similar chemical profiles (Fig. 13), with minor variations. Therefore, based on both chemical and biostratigraphical data, the most likely correlation is between the Paris Basin bentonite (Htm, Sb16) and Subalpine Basin bentonite Mbo. To confirm this correlation, a statistical discriminant method was used (Huff, 1983; Cullen-Lollis & Huff, 1986).

Discriminant function analysis

A multivariate statistical method, discriminant function analysis, was used to analyse 26 variables (chemical elements) and four groups (bentonite beds). The discriminant analysis method was selected because it seeks to distinguish statistically between two or more groups of samples using a set of variables that are thought to differ between groups (Klecka, 1981). The mathematical objective is to weight and linearly combine the discriminating variables so that the groups are forced to be as statistically distinct as possible. Discriminant function analysis was carried out on the chemical data from 31 Oxfordian bentonite samples. The number of discriminant functions calculated is equivalent to the number of variables entered, or to one less than the number of groups (i.e. bentonite beds), whichever is smaller. Tables 4, 5 and 6 summarize the results and list the three functions, their eigenvalues and a corresponding canonical correlation coefficient. The latter is a measure of the function ability to discriminate among the groups. Values of the functions as calculated at the group means are also given. They may be thought of as defining point coordinates within a three-dimensional orthogonal grid. The eigenvalues, a measure of the relative amount of

Table 4. Summary of canonical discriminant functions: variables in the analysis.

Step		Tolerance	F to remove	Wilks' lambda
1	Cr	1·000	11·713	
2	Cr	0·556	16·901	0·618
	Ge	0·556	9·306	0·435
3	Cr	0·549	13·688	0·337
	Ge	0·531	8·892	0·264
	Hf	0·853	5·357	0·210
4	Cr	0·385	21·031	0·186
	Ge	0·503	6·506	0·093
	Hf	0·423	16·590	0·157
	Lu	0·430	11·957	0·128

variance among the group of elements accounted for by each function, indicate that the third function is relatively small compared with the first two and contributes relatively little to the discriminant analysis. The first two functions include 95·9% of the variance accounted for by the model. Moreover, the canonical correlation coefficients associated with the functions show that the first two discriminant functions are each very highly correlated with the groups and the third is somewhat less correlated.

The correlations show that the functions, especially the first two, effectively separate the four beds; different elements are important in each of the three functions. The order of importance of the elements to the discriminant model is Cr, Ge, Hf and Lu. The 31 samples were back-classified using the discriminant functions. All classified correctly in their respective groups, indicating that the discriminant functions are successful in achieving group (bed) separation. Thus, it is possible to identify a unique chemical fingerprint for each of the bentonite beds within the control group area; Fig. 14 shows the cross-plot constructed using the first two canonical discriminant functions and the positions of the samples analysed. The location of the integer for each group marks the group centroid position. Paris Basin bentonite Sb16 (4) correlates highly with the remainder of the Htm group (3) and thus is confirmed to be equivalent.

Table 6. Standardized canonical discriminant function coefficients.

	Function		
	1	2	3
Cr	1·300	−0·838	0·327
Ge	−0·304	1·174	−0·584
Hf	−1·322	−0·326	0·398
Lu	1·202	0·404	0·744

Although the biostratigraphic data and comparison of geochemical patterns (Fig. 13) suggest a possible correlation between the Mbo bentonite of the Subalpine Basin and the Paris Basin bentonite, the statistical analysis does not confirm their equivalence. However, alteration of the geochemical signal in the Mbo bentonite as a result of burial diagenesis in the Subalpine Basin may explain this apparent anomaly.

Magmatic affinities and geodynamic implications

Magmatic affinities and volcanotectonic setting

Elements that are relatively immobile during alteration of ashfall (e.g. Ti, Zr, Y and Nb) are usually used to determine the original volcanic ash composition and associated magma type. The discrimination diagram of Winchester & Floyd (1977), based on Zr/TiO_2 for the index of alkalinity, and Nb/Y for the differentiation index ratios, is routinely applied to bentonites (Merriman & Roberts, 1990; Huff *et al.*, 1993; Spears *et al.*, 1999), and permits the classification of the differentiation products of subalkaline and alkaline magma series. However, Clayton *et al.* (1996) and Spears *et al.* (1999) have shown that such discrimination diagrams must be used with caution, especially when elemental concentrations are low. Ratios of Zr/TiO_2 and Nb/Y are highly dependent on the abundance of heavy minerals (zircon, anatase, rutile, ilmenite, monazite).

Table 5. Eigenvalues of discriminant function analysis.

Function	Eigenvalue	Percentage variance	Cumulative percentage	Canonical correlation
1	6·767*	82·8	82·8	0·933
2	1·329*	16·3	99·0	0·755
3	0·081*	1·0	100·0	0·274

*First three canonical discriminant functions were used in the analysis.

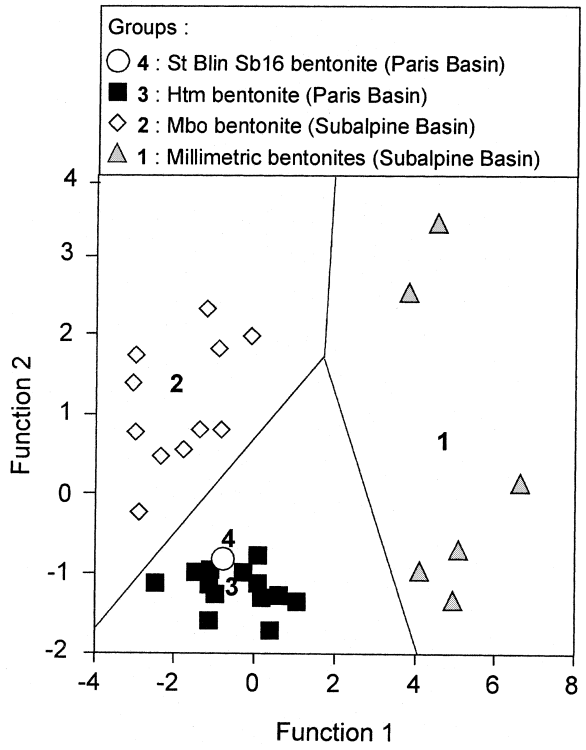

Fig. 14. Discriminant functions plot showing the separation of samples from (1) millimetric bentonites, (2) bentonite Mbo, (3) bentonite Htm, and the correspondence between (4) bentonite Sb16 and the Htm group.

These minerals can be concentrated in bentonite deposits either because of fractionation during aeolian transport or water settling, or because of mixing with enclosing detrital shales containing zircon and other heavy minerals inherited from a protolith.

The analyses plotted on such a Winchester & Floyd diagram overlap three magmatic fields: andesite, trachyandesite and basanite/nephelinite (Fig. 15A). One group that is closely clustered corresponds to bentonites B1, B3 and B5 Oze and plots close to the andesite/trachyandesite boundary, whereas another group, corresponding to bentonites Htm, Sb16 and Mbo, plots close to the trachyandesite/basanite–nephelinite boundary. These groupings help to confirm that bentonites Htm, Sb16 and Mbo may correspond to the same volcanic event. Bentonite B2 exhibits a more basic character (basanite/nephelinite).

Mineralogical and geochemical data indicate that the thin bentonites B1, B2, B3 and B5 are probably significantly contaminated by detrital sediments. Paris Basin bentonites Sb16 and Htm do not show a pronounced admixture and have been less affected by diagenesis. Therefore, an original trachyandesitic volcanic ash composition can be proposed for the Paris Basin bentonite but, to confirm this, other discrimination diagrams were investigated. Caution was exercised concerning the volcanic ash composition of bentonites from the Subalpine Basin (B1, B2, B3, B5), which contain detrital clay minerals including illite and chlorite.

The diagram of Leat *et al.* (1986) based on TiO_2 vs. Zr was used to provide information about magmatic affinities and volcanotectonic fields (Fig. 15B). Elemental values were normalized to 15% Al_2O_3 (Spears *et al.*, 1999) because concentrations are plotted rather than ratios. Al_2O_3 concentrations range between 10% and 30%. High concentrations of Al_2O_3 indicate a probable enrichment in immobile elements during alteration processes. For unaltered ashes, the concentration of Al_2O_3 depends on magmatic affinities, but the average composition of ashfalls is typically around 15% (Fisher & Schmincke, 1984). This value was used as a first approximation (Spears *et al.*, 1999) and allows the influence of the enrichment of immobile elements vs. mobile elements to be reduced. The result (Fig. 15B) seems to be consistent with the Winchester & Floyd (1977) diagram. The line A–B can be used to distinguish between basalts and intermediate-to-acid volcanics. Bentonites Htm, Sb16 and Mbo correspond to intermediate volcanic rocks and are grouped in the 'within-plate lavas' geodynamic field.

Other elements, including Tb, Th, Ta, Yb, Y, Nb and Rb, are used to construct diagrams to distinguish tectonomagmatic fields (Wood, 1980; Pearce *et al.*, 1984; Cabanis & Thiéblemont, 1988). The ratios Ta/Tb and Th/Tb, like Nb/Y, constitute good indicators of the degree of alkalinity for the source magma, while the ratio Th/Ta indicates the geodynamic context and allows separation of orogenic volcanic rocks, tholeiitic series or calc-alkaline series (Th/Ta >3·5) from intraplate magma, tholeiitic, transitional or alkaline series (Th/Ta <1·75). Bentonite trace element data were plotted on the triangular (Th–Hf/3–Ta) diagram (Fig. 15C) proposed by Wood (1980) and are grouped in two distinct closely clustered domains. Bentonites Htm, Sb16 and Mbo plotted within or close to the field of an alkaline series characteristic of within-plate or rifting (continental or oceanic) magmatism. This was confirmed by a Tb*3–Ta*2–Ta triangular diagram (Cabanis & Thiéblemont, 1988). Millimetric bentonites plot close to the field of orogenic volcanism (destructive plate margin) and suggest a different source, but again caution is necessary because of the

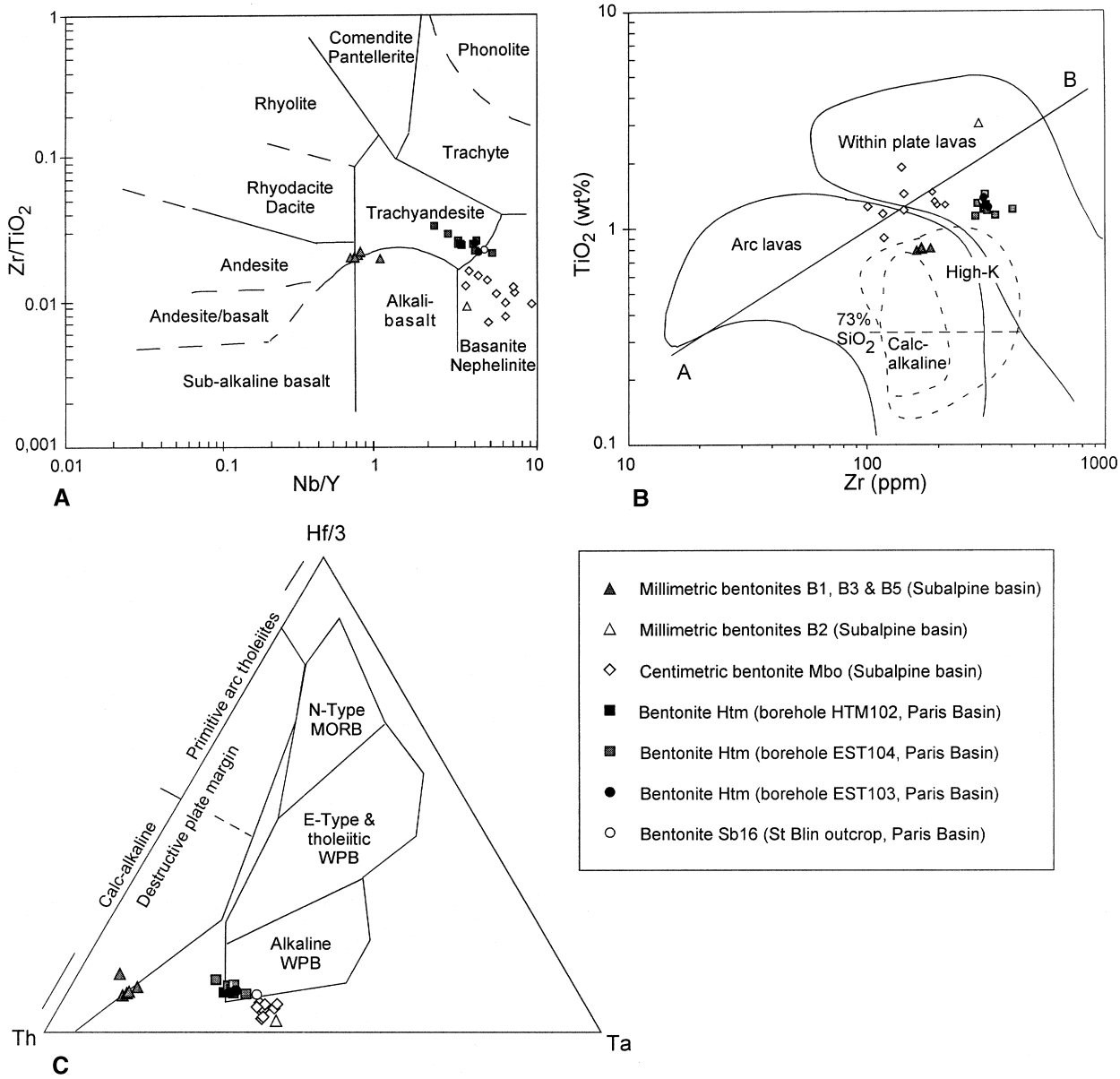

Fig. 15. Oxfordian bentonite samples (Paris and Subalpine Basins) plotted on selected magmatic or volcanotectonic setting discrimination diagrams. (A) Winchester & Floyd (1977); (B) Leat *et al.* (1986), the bentonite analyses have been normalized to 15% Al_2O_3 (see text); (C) Wood (1980).

potentially contaminated nature of these thin ash layers.

Mid-ocean ridge basalt (MORB) normalization spidergrams (modified from Pearce, 1982) provide an overall view of geochemical element distribution (Fig. 16). They are constructed based on the mobility and the incompatible nature of elements. The large ion lithophile elements (LILE), such as Sr, K, Rb and Ba, are the more mobile and are likely to be unreliable for provenance studies. In comparison with representative lavas from different tectonomagmatic domains, the Oxfordian bentonites show a similar pattern to alkalic basalts from within-plate domains (Fig. 16). High concentrations of LILE and high field strength elements (HFSE) Ta and Nb are common for most of the magmas derived from alkaline series, with more or less pronounced positive anomalies in Sm and Y. The concentration of Cr is depleted for alkalic basalts and decreases with increasing magmatic differentiation. The Cr contents of the Oxfordian bentonites are particularly low. Moreover, this diagram (Fig. 16) shows higher Th, Ta, Nb and Ce contents than alkalic basalt, suggesting differentiated products, and this is consistent with an original

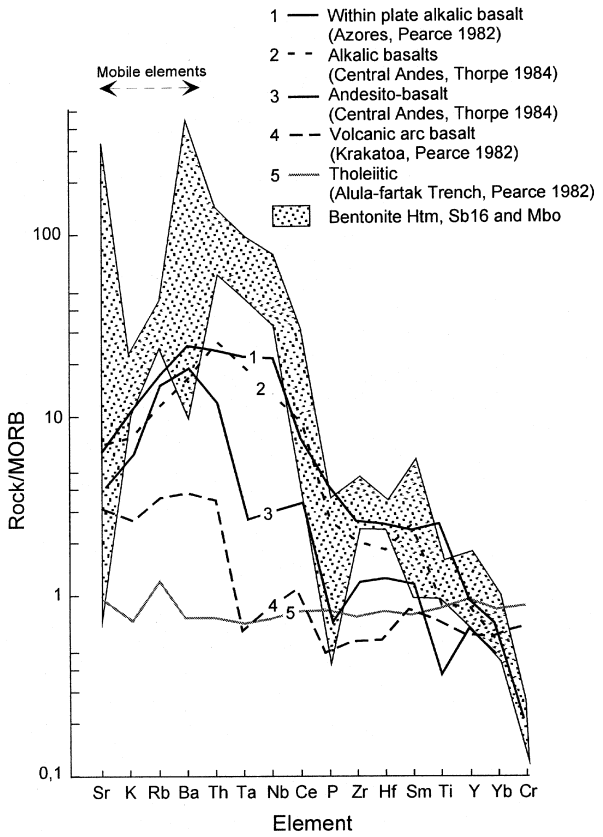

Fig. 16. MORB-normalized spidergrams for studied bentonites and comparison with volcanotectonic setting spidergrams.

trachyandesitic composition derived from a within-plate alkalic basalt. The sources cannot have been volcanics derived from orogenic settings because these are characterized by significant negative anomalies in Ta and Nb (Pearce, 1982; Cabanis & Thiéblemont, 1988). Continental tholeiites, which are marked by a strong negative anomaly in Nb (Dupuy & Dostal, 1984), must also be rejected.

REE distribution

The REE composition of volcanic ash may reflect the composition of the parental magmatic source. In bentonites, four types of processes may affect the original signature (Wray, 1995; Clayton *et al.*, 1996): (1) sorting during aeolian transport responsible for the near-vent concentration of heavy minerals (Fisher & Schmincke, 1984); (2) mixing with enclosing sediment after deposition; (3) dissolution and recrystallization reactions occurring during argillation, responsible for the removal or incorporation of REE from sea water; and (4) diagenetic processes such as oxidation–reduction reactions and fluid circulation. The Cody Shale-normalized patterns of bentonites from the Paris and Subalpine Basins (Fig. 12) display an anomalous enrichment in REE, particularly LREE. This contrasts with the patterns of shales from both basins, which are characterized by slightly negative Ce and, sometimes, negative Eu anomalies. The original chemical signature is therefore partly preserved in the bentonites.

Negative Eu and Ce anomalies are common in marine shales. A negative Ce anomaly commonly reflects the precipitation of authigenic minerals in equilibrium with sea water, whereas a negative Eu anomaly may be a function of reducing conditions in the basin (MacRae *et al.*, 1992; Wray, 1995). The absence of a negative Ce anomaly in most bentonite layers suggests that argillation of the original volcanic glass took place in a partially closed system rather than on the sea floor.

All the bentonites show high REE contents and an enrichment in LREE (Fig. 12). REE are dominantly concentrated in non-carbonate minerals, including accessory heavy minerals such as zircon and apatite, and in clay minerals. These minerals are more abundant in bentonite deposits, and this may explain their high REE contents. However, occasionally, high values may reflect the additional contribution of detrital heavy minerals in bentonite deposits (Clayton *et al.*, 1996). This may be the case in the B2 bentonite that has the highest REE content.

Enrichment of LREE from La to Sm, confirmed by a high La_N/Yb_N ratio and a relatively low La_N/Sm_N ratio, may indicate a low degree of partial melting, which is consistent with an ash derived from a parental alkaline magmatic source. REE data normalized to Cody Shale display no negative Eu anomaly, only in some cases a weak positive Eu anomaly. Wray (1995, 1999) demonstrated a systematic pronounced negative Eu anomaly in bentonites originating from rhyolitic to dacitic volcanism. A negative Eu anomaly was attributed to the removal of Eu by plagioclase feldspar during fractionation of the melt and constitutes a marker of highly evolved magmas. However, Eu distribution is also controlled during diagenesis by oxidation–reduction reactions with a loss of Eu^{2+} under highly reducing conditions and enrichment of Eu^{3+} in an oxidizing environment (MacRae *et al.*, 1992). Oxfordian shales from the Paris and Subalpine Basins display weak negative Eu anomalies, which may indicate a reducing environment consistent with the abundance of pyrite. In that case, the excess Eu in the bentonites may not result from

oxidizing conditions, but suggests a moderately evolved original magma.

Middle/Late Jurassic volcanism and sources

The volcanic sources of western European Jurassic bentonites are problematic because few nearby active volcanic centres are known for this period. Volcanoclastic deposits resulting from direct fallout of subaerially transported volcanic ash are also rarely recorded in Middle/Upper Jurassic strata (Jeans *et al.*, 2000). A submarine alkali basalt lava flow of 50 km^2 has been described in the Causses area, south of the French Central Massif, interbedded in a calcareous succession of Middle Jurassic, dated by K/Ar at 155 ± 6 Ma (Baubron *et al.*, 1978; Roux & Senaud, 1981). This submarine event is the only evidence of Jurassic volcanism in the French Central Massif and may be linked to a subaerial or submarine centre in that area. It constitutes a potential source, given the alkaline nature of this volcanism and the possibility of associated differentiated products. However, as the material of the bentonite deposits is very fine grained, the source area might be located at a greater distance.

In the Ligurian Alps, acidic submarine lavas associated with pyroclastic deposits of probable rhyodacitic composition occur in the Middle Jurassic (Cortesogno *et al.*, 1981). In the Oxfordian of the Northern Calcareous Alps, Diersche (1980) recorded more or less acidic tuffs, whereas in the Southern Alps, Bars (1965) and Sturani (1969) have described tuffites of Late Middle Jurassic age. In the same area (Altopiano di Asiago, Trento Plateau), thin intercalations of bentonites of probable trachytic to rhyolitic composition occur in the Upper Jurassic Rosso Ammonitico Superiore (Bernoulli & Peters, 1970, 1974). These layers belong to the Middle Oxfordian, *transversarium* zone (Martire, 1989; Baumgartner *et al.*, 1995). This acidic calc-alkaline volcanic material from the northern and southern Alps can be traced as far as Hungary and may be linked to the late Jurassic subduction zone of the Vardar in the Hellenids (Lemoine, 1978; Celet *et al.*, 1980). The geochemical characteristics of the Paris and Subalpine Basin bentonites (and particularly Mbo, Sb16 and Htm), however, clearly indicate an original alkaline magma, so it is unlikely that they originated from an Alpine source.

In more distant areas, volcanic activity is also recorded from the Middle and Late Jurassic. Several igneous events are identified in the Levant area of the eastern Mediterranean with basalts and more differentiated rocks ranging in composition from weakly subalkaline to alkaline compositions (Segev, 2000). All are enriched in incompatible elements (particularly LREE) and are related to rifting and hot spots or mantle plumes (Wilson *et al.*, 1998; Segev, 2000). The Jurassic volcanism in the Levant (205–161 Ma) is probably part of a large 'Western Tethyan Province' at the north of Gondwana associated with the opening of the Neotethys, now subducted. In this geodynamic context, submarine or subaerial volcanic activity is known in several areas: in western Sicily (Jenkyns, 1970), in northern Tunisia (Ziegler, 1988; Wilson *et al.*, 1998) and in the external Betic Cordillera (Ziegler, 1988). Intraplate domains of Gondwana are marked by anorogenic alkaline igneous complexes in Sudan: northern Korfodan (163 Ma) and the Bayuda desert (159 Ma). Additionally, tholeiitic and alkaline magmatism accompanied the various phases of opening of the central and equatorial Atlantic ocean (Manspeizer, 1988; Wilson *et al.*, 1998). However, these sources are probably too distant to explain the occurrence of the bentonites discussed here. Palaeogeographic reconstructions place the two areas more than 2000 km apart and, even for the most powerful known plinian or ultra-plinian eruptions, 10 cm thick ashfall deposits generally accumulate less than 2000–3000 km from the vent (Walker, 1980; Rose & Chesner, 1990; Huff *et al.*, 1996).

In the North Atlantic domain, the most intense phase of rifting occurred in latest Middle to Late Jurassic times, generating several Jurassic rift basins: East Greenland Rift; Viking Graben; Faeroe–Shetland Basin; Celtic Sea; Porcupine Basin; Jeanne d'Arc Basin; Lusitanian Basin; and probably the Rockall Trough (Ziegler, 1988; Cole & Peachey, 1999; Doré *et al.*, 1999; Roberts *et al.*, 1999). In this synrift geodynamic context, magmatic activity should be intensive and marked by diverse alkaline magmatism, including undersaturated to more acidic magmas and more highly differentiated products. However, there is little remaining evidence of this magmatism except for the North Sea, which is characterized by an important volcanic complex at the triple junction between the Viking, Central and Moray Firth rifts in the Middle Jurassic (Ziegler, 1988). From the Late Jurassic to Early Cretaceous, minor alkaline volcanic activity is recorded in onshore areas from the Lusitanian Basin and a submarine chain of volcanoes of the south-central part of the Porcupine Trough (Ziegler, 1988). In the Hebrides

Basin, Knox (1977) described three pure montmorillonite pale grey mudstone bands, interpreted as altered tuffs of basic to intermediate composition. They were assigned to the Upper Callovian/Lower Oxfordian (*athleta*, lower *cordatum* and upper *cordatum* zones) which may suggest minor volcanic activity in this area. These deposits are biostratigraphically and geochemically close to the bentonites described in the present paper, suggesting the possibility of a common origin. In the same area, Norris & Hallam (1995) described a tuff layer interbedded in Callovian clays (Staffin Shale Formation, *athleta* zone).

In the North Sea realm, smectite-rich horizons described as primary bentonites are supposed to be intimately related to synchronous North Sea volcanism. Bradshaw (1975) recorded the occurrence of bentonite deposits in the Bathonian marginal marine and lagoonal facies of eastern England, and Malm *et al.* (1979) have described a thin tuff bed in the Middle Jurassic of the Statfjord oilfield. Tuffs described in the Brent Group of the North Sea have been dated as Kimmeridgian (Howitt *et al.*, 1975). Jeans *et al.* (2000) have provisionally interpreted smectite-rich clay mineral assemblages with pronounced LREE enrichment as bentonites in the Purbeck Formation (uppermost Jurassic/lowest Cretaceous) of Durlston Bay (Dorset). These authors suggested that the source of most volcanic material in the British Jurassic must have been to the east of England in the North Sea or in adjacent regions of western Europe. In the central North Sea Jurassic volcanic centres, major activity occurred during the mid-Jurassic, which may have played an important role in the distribution of volcanogenic clay (Woodhall & Knox, 1979; Furnes *et al.*, 1982; Latin *et al.*, 1990; Smith & Ritchie, 1993).

The Middle Jurassic lavas of the Egersund subbasin display a typical geochemical pattern of strongly alkaline basalts formed by a small degree of partial melting (Furnes *et al.*, 1982), which is compatible with the studied bentonites. However, radiometric age and biostratigraphical data indicate that these centres were buried by Oxfordian time by paralic and marine sediments resulting from a series of major transgressions (Smith & Ritchie, 1993). This is also the reason why Knox (1977) suggested that the source of Callovian and Oxfordian bentonites on the Isle of Skye, NW Scotland, may originate from a zone of potential rifting to the west and north of Britain, rather than to the Jurassic volcanic centres of North Sea. Finally, a Jurassic volcanic centre covered by Lower Cretaceous sandstones has been found in the Zuidwal Basin, NW Netherlands (Cottençon *et al.*, 1975), which constitutes, along with the Forties–Piper area, the only volcanic centre known to be associated with Jurassic rifting in the North Atlantic domain. Pyroclastic breccias associated with the Zuidwal volcanic centre give an age of 152 ± 3 Ma, which is coeval with the Oxfordian bentonites. In addition, geochemical characteristics of the pyroclastic rocks are consistent with the chemical data of the bentonites described in this paper (Lacharpagne, 1986). Therefore, it is concluded that this volcanic centre likely constitutes the source of ashes deposited in the Paris and Subalpine Basins.

CONCLUSIONS

The occurrence of bentonites in Middle Oxfordian deposits of the Paris and Subalpine Basins indicates that significant volcanic activity occurred during the Late Jurassic. Bentonites may be identified on the basis of field characteristics, bulk mineralogy (abundance of euhedral crystals of zircon, amphibole, apatite and feldspar), clay mineralogy (pure smectite horizons or mixtures of kaolinite and I/S mixed layer) and geochemistry (enrichment in Hf, Nb, Pb, Ta, Th, Ti, U, Y and Zr), that differ greatly from the enclosing shales.

A single bentonite layer occurs in the eastern part of the Paris Basin, and this can be correlated from continuously cored boreholes to an outcrop located 20 km to the south. This layer is composed of dioctahedral smectite (95%) with minor proportions of kaolinite, chlorite and illite, indicating mixing with the host sediments, probably caused by bioturbation.

In the Subalpine Basin, five bentonite horizons have been identified. These are characterized by a mixture of kaolinite and regular or random illite/smectite mixed layers. In this basin, burial diagenesis and fluid migration were probably responsible for the observed mineralogy. Fluid migration also caused sulphate–carbonate mineralization at the base of the thickest bentonite. Four thin bentonites have mineralogical and geochemical compositions that reveal significant contamination by associated sediments, but the thickest bentonite (Mbo) is little affected by mixing with the enclosing shales. The thin bentonites can be partially correlated from section to section. However, bentonite Mbo, occurring in

the *vertebrale* subzone (Middle Oxfordian), has been correlated between 10 sections, covering 2000 km^2 of the basin.

According to the biostratigraphic and geochemical data, bentonite Mbo may be a lateral equivalent of the bentonite layer identified in the Paris Basin, although the correlation could not be confirmed by statistical analysis of the geochemical data. This layer may offer a long-distance isochronous correlation line between both basins and offers the possibility of radiometric dating.

Immobile trace element chemistry indicates a trachyandesitic composition for the original ash derived from an alkaline series in an intraplate volcanotectonic setting. The Oxfordian bentonites probably derive from the weathering of ashes originating from the Zuidwal (NW Netherlands) active volcanic centre.

ACKNOWLEDGEMENTS

The authors acknowledge Professor D. A. Spears and Dr D. S. Wray for constructive reviews, Editor Dr I. Jarvis and Dr S. P. Hesselbo for useful comments provided on the original manuscript.

REFERENCES

Andra (2000) *Recherches pour le Stockage des Déchets Radioactifs à Haute Activité et à Vie Longue.* Bilan des études et travaux 2000. Collection les rapports, 544 pp.

Artru, P. (1972) *Les Terres Noires du Bassin Rhodanien (Bajocien supérieur à Oxfordien moyen) – Stratigraphie, Sédimentologie, Géochimie*. PhD Thesis, Université de Lyon, 173 pp.

Bars, H. (1965) Geologie des südlichen Nonsberges und der angrenzenden Gebiete. *Veröff. Mus. Fredinandeum*, **45,** 5–60.

Batchelor, R.A. and **Jeppsson, L.** (1999) Wenlock metabentonites from Gotland, Sweden: geochemistry, sources and potential as chemostratigraphic markers. *Geol. Mag.*, **136,** 661–669.

Baubron, J.C., Defaut, B., Demange, J. and **Maury, R.C.** (1978) Une coulée sous-marine d'âge jurassique moyen dans les Causses: le basalte alcalin des Vignes (Massif Central français). *CR Acad. Sci. Paris*, **287,** 225–227.

Baumgartner, P.O., O'Dogherty, L., Gorican, S., Urquhart, E., Pillevuit, A. and **De Wever, P.** (1995) Middle Jurassic to Lower Cretaceous radiolaria of Tethys: occurrences, systematics, biochronology. *Géol. Mém. Lausanne*, **23,** 737–745.

Bernoulli, D. and **Peters, T.** (1970) Traces of rhyolitic-trachytic volcanism in the Upper Jurassic of the Southern Alps. *Eclogae Geol. Helv.*, **63,** 609–621.

Bernoulli, D. and **Peters, T.** (1974) Traces of rhyolitic-trachytic volcanism in the Upper Jurassic of the Southern Alps: Reply. *Eclogae Geol. Helv.*, **67,** 209–213.

Bohor, B.F. and **Triplehorn, D.M.** (1993) Tonsteins: altered volcanic-ash layers in coal-bearing sequences. *Geol. Soc. Am. Spec. Paper*, **285,** 1–44.

Borchardt, G.A., Harward, M.E. and **Schmitt, R.A.** (1971) Correlation of volcanic ash deposits by activation analysis of glass separates. *Quatern. Res.*, **1,** 247–260.

Bradshaw, M.J. (1975) Origin of montmorillonite bands in the Middle Jurassic of Eastern England. *Earth Planet. Sci. Lett.*, **26,** 245–252.

Brown, G. and **Brindley, G.W.** (1980) X-ray procedures for clay mineral identification. In: *Crystal Structures of Clay Minerals and Their X-Ray Identification* (Eds G.W. Brindley and G. Brown), pp. 305–359. Mineralogical Society, London.

Cabanis, B. and **Thiéblemont, D.** (1988) La discrimination des tholéiites continentales et des basaltes arrière-arc. Proposition d'un nouveau diagramme, le triangle Th-3 × Tb-2 × Ta. *Bull. Soc. Géol. Fr.*, **6,** 927–935.

Celet, P., Clément, B., Ferrière, J. and **Thiébault, F.** (1980) Tableau des principaux évènements tectoniques, métamorphiques et magmatiques dans les Hellénides au cours du cycle alpin. In: *Colloque C5 Geology of the Alpine Chains Born of the Tethys* (Eds J. Aubouin, J. Debelmas and M. Latreille), *26 CGI, Bur. Rech. Géol. Min. Mém.*, **115,** 306–307.

Clayton, T., Francis, J.E., Hillier, S.J., Hodson, F., Saunders, R.A. and **Stone, J.** (1996) The implications of reworking on the mineralogy and chemistry of the Lower Carboniferous K-bentonites. *Clay Mineral.*, **31,** 377–390.

Cole, J. and **Peachey, J.** (1999) Evidence for pre-Cretaceous rifting in the Rockall Trough: a quantitative analysis using plate tectonic modelling. In: *Petroleum Geology of Northwest Europe, 1* (Eds J. Fleet and S.A.R. Boldy), pp. 359–370. Geological Society, London.

Collin, P.Y. and **Courville, P.** (2000) Paléoenvironnements et biostratigraphie d'une série oxfordienne non condensée de référence (Saint-Blin-Sémilly, Haute-Marne, France). *Géol. Fr.*, **1,** 59–63.

Cortesogno, L., Oxilia, M., Royant, G., Vanossi, M. and **Vivier, G.** (1981) Témoins d'un volcanisme rhyodacitique du Dogger dans le domaine prépiémontais des Alpes ligures. *Eclogae Geol. Helv.*, **74/3,** 569–585.

Cottençon, A., Parant, B. and **Flacelière, G.** (1975) Lower Cretaceous gas-fields in Holland. In: *Petroleum and the Continental Shelf of North-West Europe* (Ed. A.W. Woodland), *Geology*, **1,** 403–412.

Cullen-Lollis, J. and **Huff, W.D.** (1986) Correlation of Champlainian (Middle Ordovician) K-bentonite beds in Central Pennsylvania based on chemical fingerprinting. *J. Geol.*, **94,** 865–874.

Debrabant, P., Chamley, H., Deconinck, J.F., Récourt, P. and **Trouiller, A.** (1992) Clay sedimentology, mineralogy and chemistry of Mesozoic sediments drilled in the Northern Paris Basin. *Sci. Drilling*, **3,** 138–152.

Debrand-Passard, S., Enay, R., Rioult, M., Cariou, E., Marchand, D. and **Menot, J.C.** (1980) Jurassique supérieur. In: *Synthèse Géologique du Bassin de Paris. II. Stratigraphie et Paléogéographie* (Eds C. Mégnien and F. Mégnien), *Bur. Rech. Géol. Min. Mém.*, **101,** 195–253.

Debrand-Passard, S., Courbouleix, S. and **Lienhardt, M.J.** (1984) Synthèse géologique du Sud-Est de la France. *Bur. Rech. Géol. Min. Mém.*, **125,** 614 pp.

Deconinck, J.F. (1987) Identification de l'origine détritique ou diagénétique des assemblages argileux: le cas des alternances marne-calcaire du Crétacé inférieur subalpin. *Bull. Soc. Géol. Fr.*, **3,** 139–145.

Deconinck, J.F. and **Chamley, H.** (1995) Diversity of smectite origins in Late Cretaceous sediments: example of chalks from northern France. *Clay Mineral.*, **30,** 365–379.

Deconinck, J.F. and **Debrabant, P.** (1985) Diagenèse des argiles dans le domaine subalpin: rôles respectifs de la lithologie, de l'enfouissement et de la surcharge tectonique. *Rev. Géol. Dynam. Géog. Phys.*, **26/5,** 321–330.

Deconinck, J.F., Amédro, F., Robaszynski, F., Pellenard, P. and **Récourt, P.** (2000) Influences détritiques et volcaniques sur la minéralogie de la fraction argileuse des formations crayeuses traversées par le forage de Poigny (projet craie 700). Résultats préliminaires. *Bull. Inf. Géol. Bassin Paris*, **37,** 107–111.

Diersche, V. (1980) Die Radiolarite des Oberjura im Mittelabschnitt der Nördlichen Kalkalpen. *Geotekton. Forsch.*, **58,** 1–217.

Doré, A.G., Lundin, E.R., Jensen, L.N., Birkelund, Ø., Eliassen, P.E. and **Fichler, C.** (1999) Principal tectonic events in the evolution of the northwest European Atlantic margin. In: *Petroleum Geology of Northwest Europe, 1* (Eds J. Fleet and S.A.R. Boldy), pp. 41–62. Geological Society, London.

Dugué, O. (1991) Comportement d'une bordure de massifs anciens et cortèges de minéraux argileux: l'exemple de la bordure occidentale du Bassin Anglo-Parisien au Callovo-Oxfordien. *Palaeogeogr. Palaeoclimatol. Palaeoecol.*, **81,** 323–346.

Dupuy, C. and **Dostal, J.** (1984) Trace element geochemistry ofsome continental tholeiites. *Earth Planet. Sci. Lett.*, **67,** 61–69.

Evensen, N., Hamilton, P.J. and **O'Nions, R.K.** (1978) Rare-earth abundances in chondrite meteorites. *Geochim. Cosmochim. Acta*, **42,** 199–212.

Fisher, R.V. and **Schmincke, H.U.** (1984) *Pyroclastic Rocks*. Springer-Verlag, Berlin, 472 pp.

Fortwengler, D. (1989) Biostratigraphie des Terres Noires d'âge Callovien supérieur à Oxfordien moyen des chaînes subalpines du Sud (Diois, Baronnies, Dévoluy). *CR Acad. Sci. Paris*, **308,** 531–536.

Furnes, H., Elvsborg, A. and **Malm, O.A.** (1982) Lower and Middle Jurassic alkaline magmatism in the Egersund subbasin, North Sea. *Mar. Geol.*, **46,** 53–69.

Gaidon, J.M. (1988) *Minéralisation et structuration d'une marge continentale passive: l'exemple des concrétions tubulaires du bassin subalpin (Callovien-Oxfordien)*. PhD Thesis, Université de Lyon I, 222 pp.

de Graciansky, P.C., Dardeau, G., Bodeur, Y., Elmi, S., Fortwengler, D., Jacquin, T., Marchand, D. and **Thierry, J.** (1999) Les Terres Noires du Sud-Est de la France (Jurassique moyen et supérieur) interprétation en termes de stratigraphie séquentielle. *Bull. Centres Rech. Explor.-Prod. Elf-Aquitaine*, **22,** 35–69.

Guilhaumou, N., Touray, J.C., Perthuisot, V. and **Roure, F.** (1996) Paleocirculation in the basin of southeastern France subalpine range: a synthesis from fluid inclusions studies. *Mar. Petrol. Geol.*, **13,** 695–706.

Howitt, F., Aston, E.R. and **Jacqué, M.** (1975) The occurrence of Jurassic volcanics in the North Sea. In: *Petroleum and the Continental Shelf of North-West Europe, Geology* (Ed. A.W. Woodland), *Geology*, **1,** 379–386.

Huff, W.D. (1983) Correlation of Middle Ordovician K-bentonites based on chemical fingerprinting. *J. Geol.*, **91,** 657–669.

Huff, W.D. and **Kolata, D.R.** (1990) Correlation of the Ordovician Deicke and Millbrig K-bentonites between the Mississippi valley and the southern Appalachians. *AAPG Bull.*, **74,** 1736–1747.

Huff, W.D., Merriman, R.J., Morgan, D.J. and **Roberts, B.** (1993) Distribution and tectonic setting of Ordovician K-bentonites in the United Kingdom. *Geol. Mag.*, **130,** 93–100.

Huff, W.D., Kolata, D.R., Bergström, S.M. and **Zhang, Y.S.** (1996) Large-magnitude Middle Ordovician volcanic ash falls in North America and Europe: dimensions, emplacement and post-emplacement characteristics. *J. Volcanol. Geoth. Res.*, **73,** 285–301.

Inoue, A., Bouchet, A., Velde, B. and **Meunier, A.** (1989) Convenient technique for estimating smectite layer percentage in randomly interstratified illite/smectite minerals. *Clay Clay Mineral.*, **37,** 227–234.

Jarvis, I. and **Jarvis, K.E.** (1985) Rare-earth element geochemistry of standard sediments: a study using inductively coupled plasma spectrometry. *Chem. Geol.*, **53,** 335–344.

Jeans, C.V., Wray, D.S., Merriman, R.J. and **Fisher, M.J.** (2000) Volcanogenic clays in Jurassic and Cretaceous strata of England and the North Sea Basin. *Clay Mineral.*, **35,** 25–55.

Jenkyns, H.C. (1970) Submarine volcanism and the Toarcian iron pisolites of Western Sicily. *Eclogae Geol. Helv.*, **63,** 549–572.

Klecka, W.R. (1981) Discriminant analysis. In: *SPSS: Statistical Package for the Social Sciences*, 2nd edn (Eds N.H. Nie, C.H. Hull, J.G. Jenkins, K. Steinbrenner and D.H. Bent), pp. 434–467. McGraw-Hill, New York.

Knox, R.W.O.B. (1977) Upper Jurassic pyroclastic rocks in Skye, West Scotland. *Nature*, **265,** 323–324.

Kolata, D.R., Frost, J.K. and **Huff, W.D.** (1987) Chemical correlation of K-bentonite beds in the Middle Ordovician Decorah Subgroup, Upper Mississippi Valley. *Geology*, **15,** 208–211.

Kolata, D.R., Huff, W.D. and **Bergström, S.M.** (1996) Ordovician K-bentonites of eastern North America. *Geol. Soc. Am. Spec. Paper*, **313,** 84.

Lacharpagne, J.C. (1986) *Zuidwal 1 (Hollande). Etude Géochimique du Volcanisme*. Unpubl. report. Elf-Aquitaine, pp. 1–10.

Latin, D.M., Dixon, J.E. and **Fitton, J.G.** (1990) Rift-related magmatism in the North Sea Basin. In: *Tectonic Evolution of the North Sea Rifts* (Eds D.H. Blundell and A.D. Gibbs), pp. 101–104. Clarendon Press, Oxford.

Leat, P.T., Jackson, S.E., Thorpe, R.S. and **Stillman, C.J.** (1986) Geochemistry of bimodal basalt-sub-alkaline/peralkaline provinces within the southern British Caledonids. *J. Geol. Soc. London*, **141,** 259–273.

Lefrançois, A., Marchand, D., Beaudoin, B., Chamley, H. and **Trouiller, A.** (1996) Contexte géodynamique au passage Callovien-Oxfordien dans le NNE du Bassin Parisien. *CR Acad. Sci. Paris*, **323,** 229–235.

Lemoine, M. (1978) *Geological Atlas of Alpine Europe*. Elsevier, Amsterdam, 584 pp.

Lemoine, M. and **de Graciansky, P.C.** (1988) Marge continentale téthysienne dans les Alpes. *Bull. Soc. Géol. Fr.*, **4,** 598–797.

Levert, J. and **Ferry, S.** (1988) Diagenèse argileuse complexe dans le Mésozo subalpin révélée par cartographie des proportions relatives d'argiles selon des niveaux isochrones. *Bull. Soc. Géol. Fr.*, **4,** 1029–1038.

MacRae, N.D., Nesbitt, H.W. and **Kronberg, B.I.** (1992) Development of a positive Eu anomaly during diagenesis. *Earth Planet. Sci. Lett.*, **109,** 585–591.

Malm, O.A., Furnes, H. and **Bjørlykke, K.** (1979) Volcanoclastics of Middle Jurassic age in the Statford oil-field of the North Sea. *Neues Jb. Geol. Paläontol. Monat.*, **10,** 607–618.

Manspeizer, W. (1988) *Triassic–Jurassic Rifting. Continental Break-Up and the Origin of the Atlantic Ocean and Passive Margins.* Elsevier, Amsterdam, 998 pp.

Marchand, D., Fortwengler, D., Dardeau, G., de Graciansky, P.C. and **Jacquin, T.** (1990) Les peuplements d'ammonites du Bathonien supérieur à l'Oxfordien moyen dans les Baronnies (bassin du sud-est, France): comparaison avec la plate-forme Nord-Européenne. *Bull. Centres Rech. Explor.-Prod. Elf-Aquitaine*, **14,** 465–479.

Martire, L. (1989) *Analisi biostratigrafica e sedimentologica del Rosso Ammonitico Veronese dell'Altopiano di Asiago (VI).* PhD Thesis, Università di Torino, 166 pp.

Merriman, R.J. and **Roberts, B.** (1990) Metabentonites in the Moffat Shale Group, Southern Uplands of Scotland: geochemical evidence of ensialic marginal basin volcanism. *Geol. Mag.*, **127,** 259–271.

Moore, D.M. and **Reynolds, R.C.** (1997) *X-ray Diffraction and the Identification and Analysis of Clay Minerals*, 2nd edn. Oxford University Press, Oxford.

Norris, M. and **Hallam, A.** (1995) Facies variations across the Middle–Upper Jurassic boundary in Western Europe and the relationship to sea-level changes. *Palaeogeogr. Palaeoclimatol. Palaeoecol.*, **116,** 189–245.

Pacey, N.R. (1984) Bentonites in the Chalk of central eastern England and their relation to the opening of northeast Atlantic. *Earth Planet. Sci. Lett.*, **67,** 48–60.

Pearce, J.A. (1982) Trace element characteristics of lavas from destructive plate boundaries. In: *Andesites. Orogenic Andesites and Related Rocks* (Ed. R.S. Thorpe), pp. 525–549. Wiley, Chichester.

Pearce, J.A., Harris, N.B.W. and **Tindle, A.G.** (1984) Trace element discrimination diagrams for the tectonic interpretation of granite rocks. *J. Petrol.*, **25,** 956–983.

Pellenard, P., Deconinck, J.F., Marchand, D., Thierry, J., Fortwengler, D. and **Vigneron, G.** (1999) Contrôle géodynamique de la sédimentation argileuse du Callovien-Oxfordien moyen dans l'Est du Bassin de Paris: influence eustatique et volcanique. *CR Acad. Sci. Paris*, **328,** 807–813.

Petschick, R. (2000) *MacDiff 4.1.2. Powder Diffraction Software.* Available from the author at http://www.geol.uni-erlangen.de/html/software/Macdiff.html.

Randle, K., Goles, G.G. and **Kittleman, L.R.** (1971) Geochemical and petrological characterization of ash samples from Cascade Range volcanoes. *Quatern. Res.*, **1,** 261–282.

Reynolds, R.C. (1980) Interstratified clay minerals. In: *Crystal Structures of Clay Minerals and their X-ray Identification* (Eds G.W. Brindley and G. Brown), pp. 249–303. Mineralogical Society, London.

Roberts, B. and **Merriman, R.J.** (1990) Cambrian and Ordovician metabentonites and their relevance to the origins of associated mudrocks in the northern sector of the Lower Palaeozoic Welsh marginal basin. *Geol. Mag.*, **127,** 31–43.

Roberts, D.G., Thompson, M., Mitchener, B., Hossack, J., Carmichael, S. and **Bjørnseth, H.M.** (1999) Palaeozoic to Tertiary rift and basin dynamics: mid-Norway to the Bay of Biscay – a new context for hydrocarbon prospectivity in the deep water frontier. In: *Petroleum Geology of Northwest Europe 1* (Eds J. Fleet and S.A.R. Boldy), pp. 7–40. Geological Society, London.

Rose, W.I. and **Chesner, C.A.** (1990) Worldwide dispersal of ash and gases from earth's largest known eruption: Toba, Sumatra, 75 ka. *Palaeogeogr. Palaeoclimatol. Palaeoecol.*, **89,** 269–275.

Roux, J. and **Senaud, G.** (1981) L'anomalie magnétique des Vignes (Gorges du Tarn, Massif Central français). Mise en évidence de l'extension d'un épanchement volcanique jurassique. *Bull. Soc. Géol. Fr.*, **7,** 45–50.

Segev, A. (2000) Synchronous magmatic cycles during the fragmentation of Gondwana: radiometric ages from the Levant and other provinces. *Tectonophysics*, **325,** 257–277.

Smith, K. and **Ritchie, J.D.** (1993) Jurassic volcanic centres in the Central North Sea. In: *Petroleum Geology of Northwest Europe: Proceedings of the 4th Conference* (Ed. J.R. Parker), pp. 519–531. Geological Society, London.

Spears, D.A. (1970) A kaolinite mudstone (tonstein) in the British Coal Measures. *J. Sed. Petrol.*, **40,** 386–394.

Spears, D.A., Kanaris-Sotiriou, R., Riley, N. and **Krause, P.** (1999) Namurian bentonites in the Pennine Basin, UK – origin and magmatic affinities. *Sedimentology*, **46,** 385–401.

Sturani, C. (1969) Intercalazione di vulcaniti Medio-Giurassiche nel 'Rosso Ammonitico' dei Lessini veronesi. *Boll. Soc. Geol. Ital.*, **88,** 589–601.

Teale, C.T. and **Spears, D.A.** (1986) The mineralogy and origin of some Silurian bentonites, Welsh Borderland, UK. *Sedimentology*, **33,** 757–765.

Thorpe, R.S., Francis, P.W. and **O'Callaghan, L.** (1984) Relative roles of source composition, fractional crystallization and crustal contamination in the petrogenesis of Andean volcanic rocks. *Phil. Trans. R. Soc. London*, **310,** 675–682.

Tribovillard, N.P. (1989) Contrôle de la sédimentation marneuse en milieu pélagique semi-anoxique. Exemples dans le Mésozo du Sud-Est de la France et de l'Atlantique. *Doc. Lab. Lyon*, **109,** 119.

Walker, G.P.L. (1980) The Taupo pumice: product of the most powerful know (ultraplinian) eruption. *J. Volcanol. Geoth. Res.*, **8,** 69–94.

Westgate, J.A., Christiansen, E.Q. and **Boellstorff, J.D.** (1977) Wascana Creek ash (Middle Pleistocene) in southern Saskatchewan: Characterization, source, fission track age, paleomagnetism and stratigraphic significance. *Can. J. Earth Sci.*, **14,** 357–374.

Wilson, M., Guiraud, R., Moreau, C. and **Bellion, Y.J.C.** (1998) Late Permian to Recent magmatic activity on the African-Arabian margin of Tethys. In: *Petroleum Geology of North Africa* (Eds D.S. Macgregor, R.T.J. Moody and D.D. Clark-Lowes), *Geol. Soc. London Spec. Publ.*, **132,** 231–263.

Winchester, J.A. and **Floyd, P.A.** (1977) Geochemical discrimination of different magma series and their differentiation products using immobile elements. *Chem. Geol.*, **20,** 325–343.

Wood, D.A. (1980) The application of a Th-Hf-Ta diagram to problems of tectonomagmatic classification and to establishing the nature of crustal contamination of basaltic lavas of the British Tertiary Volcanic Province. *Earth Planet. Sci. Lett.*, **50,** 11–30.

Woodhall, D. and **Knox, R.W.O.B.** (1979) Mesozoic volcanism in the northern North Sea and adjacent areas. *Bull. Geol. Surv. Great Brit.*, **70,** 57–69.

Wray, D.S. (1995) Origin of clay-rich beds in Turonian chalks from Lower Saxony, Germany – a rare earth element study. *Chem. Geol.*, **119,** 161–173.

Wray, D.S. (1999) Identification and long-range correlation of bentonites in Turonian-Coniacian (Upper Cretaceous) chalks of northwest Europe. *Geol. Mag.*, **136,** 361–371.

Ziegler, P.A. (1988) Evolution of the Arctic-North Atlantic and the Western Tethys. *AAPG Mem.*, **43,** 198 pp.

Manuscript received 6 March 2002;
revision accepted 18 June 2003.